

ATTACHMENT

Structural Integrity Associates, Inc. Report No. 0900090.401, Revision 0

***60-Year EAF Analyses Summary Report - Kewaunee Power Station - Charging
Nozzle and RCS Hot Leg Surge Nozzle***

Dated May 2010

**KEWAUNEE POWER STATION
DOMINION ENERGY KEWAUNEE, INC.**

Report No. 0900090.401
Revision 0
Project No. 0900090
May 2010

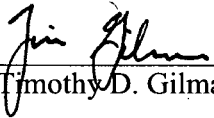
60-YEAR EAF ANALYSES SUMMARY REPORT
Kewaunee Power Station
Charging Nozzle and
RCS Hot Leg Surge Nozzle

Prepared for:

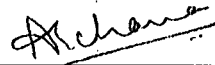
Dominion Energy Kewaunee, Inc.
Kewaunee, WI
P.O. No. 70199431, Rev. 2

Prepared by:

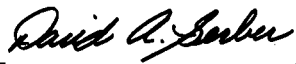
Structural Integrity Associates, Inc.
San Jose, California

Prepared by: 
Timothy D. Gilman

Date: May 11, 2010

Reviewed by: 
Archana Chinthapalli

Date: May 12, 2010

Approved by: 
David A. Gerber

Date: May 12, 2010

REVISION CONTROL SHEET

Document Number: **0900090.401**

Title: **60-YEAR EAF ANALYSES SUMMARY REPORT, Kewaunee Power Station,
Charging Nozzle and RCS Hot Leg Surge Nozzle**

Client: **Dominion Energy Kewaunee, Inc.**

SI Project Number: **0900090**

Quality Program: ☒ Nuclear ☐ Commercial

Section	Pages	Revision	Date	Comments
1.0	1-1	0	5/11/2010	Initial Issue
2.0	2-1			
3.0	3-1 – 3-4			
4.0	4-1 – 4-28			
5.0	5-1 – 5-39			
6.0	6-1			
7.0	7-1 – 7-3			



Structural Integrity Associates, Inc.

Table of Contents

<u>Section</u>	<u>Page</u>
1.0 ACRONYMS	1-1
2.0 BACKGROUND AND REPORT OBJECTIVE.....	2-1
3.0 ANALYSIS CRITERIA AND METHODOLOGY	3-1
3.1 ASME Code Fatigue Calculations	3-1
3.2 EAF Calculations	3-3
4.0 CHARGING NOZZLE	4-1
4.1 Component Description and Finite Element Model	4-1
4.2 Loading Definitions and Loading Combinations.....	4-5
4.2.1 Sources of Information for Design Transients.....	4-5
4.2.2 Operating Parameters and System Transients Considered.....	4-6
4.2.3 Transient Lumping.....	4-8
4.2.4 Heat Transfer Coefficients.....	4-8
4.2.5 Piping Interface Loads.....	4-10
4.3 Thermal and Mechanical Analyses.....	4-12
4.3.1 Methodology Overview.....	4-12
4.3.2 Boundary Conditions	4-13
4.3.3 Internal Pressure Analysis.....	4-17
4.3.4 Piping Interface Loading Analysis.....	4-18
4.3.5 Thermal Transients	4-20
4.3.6 Selection of Analysis Sections (Paths)	4-20
4.3.7 Summary of FEA Analyses.....	4-22
4.4 ASME Code Fatigue Calculations	4-24
4.4.1 Fatigue Calculations.....	4-24
4.4.2 EAF Calculations.....	4-28



5.0	RCS HOT LEG SURGE NOZZLE.....	5-1
5.1	Component Description and Finite Element Model	5-1
5.2	Loading Definitions and Loading Combinations.....	5-5
5.2.1	<i>Sources of Information for Design Transients.....</i>	<i>5-5</i>
5.2.2	<i>Operating Parameters and System Transients Considered.....</i>	<i>5-6</i>
5.2.3	<i>Transient Lumping.....</i>	<i>5-11</i>
5.2.4	<i>Heat Transfer Coefficients.....</i>	<i>5-13</i>
5.2.5	<i>Piping Interface Loads.....</i>	<i>5-15</i>
5.3	Thermal and Mechanical Analyses.....	5-16
5.3.1	<i>Methodology Overview.....</i>	<i>5-16</i>
5.3.2	<i>Boundary Conditions.....</i>	<i>5-17</i>
5.3.3	<i>Internal Pressure Analysis.....</i>	<i>5-20</i>
5.3.4	<i>Piping Interface Loading Analysis.....</i>	<i>5-21</i>
5.3.5	<i>Thermal Transients.....</i>	<i>5-22</i>
5.3.6	<i>Selection of Analysis Sections (Paths).....</i>	<i>5-22</i>
5.3.7	<i>Summary of FEA Analyses.....</i>	<i>5-26</i>
5.4	ASME Code Fatigue Calculations	5-28
5.4.1	<i>Fatigue Calculations.....</i>	<i>5-28</i>
5.4.2	<i>EAF Calculations.....</i>	<i>5-35</i>
6.0	CONCLUSIONS.....	6-1
7.0	REFERENCES.....	7-1



List of Tables

<u>Table</u>	<u>Page</u>
Table 4-1. Charging Nozzle Material Designations	4-1
Table 4-2. Charging Nozzle Material Properties	4-4
Table 4-3. Charging Nozzle Transients	4-7
Table 4-4. Summary of Charging Nozzle Heat Transfer Coefficients, Btu/hr-ft ² -°F	4-10
Table 4-5. Charging Nozzle Branch Piping Interface Loads	4-10
Table 4-6. Summary of ANSYS Load Cases	4-23
Table 4-7. Charging Nozzle Load Sets as Input to VESLFAT (PATH2)	4-25
Table 4-8. Charging Nozzle Material Properties for Fatigue Analysis	4-26
Table 4-9. Charging Nozzle Stainless Steel Fatigue Curve for Fatigue Analysis	4-27
Table 4-10. Charging Nozzle Fatigue Usage Results (no OBE)	4-27
Table 4-11. Charging Nozzle Detailed CUF Results for Bounding PATH2 (+OBE)	4-28
Table 5-1. RCS Hot Leg Surge Nozzle Material Designations	5-1
Table 5-2. RCS Hot Leg Surge Nozzle Material Properties	5-4
Table 5-3. RCS Transients for Hot Leg Surge Nozzle	5-9
Table 5-4. I/O/stratification Cycles for Pre-MOP Period	5-10
Table 5-5. I/O/stratification Cycles for Post-MOP Period	5-10
Table 5-6. Summary of All I/O/stratification Transients	5-11
Table 5-7. Summary of All RCS Hot Leg Surge Nozzle Transients to be Analyzed	5-13
Table 5-8. Summary of RCS Hot Leg Surge Nozzle Heat Transfer Coefficients, Btu/hr-ft ² -°F	5-15
Table 5-9. RCS Hot Leg Surge Nozzle Piping Interface Loads, in-kips	5-15
Table 5-10. Summary of RCS Hot Leg Surge Nozzle ANSYS Load Cases	5-27
Table 5-11. Hot Leg Surge Nozzle Load Sets as Input to VESLFAT	5-29
Table 5-12. RCS Hot Leg Surge Nozzle Material Properties for Fatigue Analysis	5-30
Table 5-13. RCS Hot Leg Surge Nozzle Stainless Steel Fatigue Curve for Fatigue Analysis	5-30
Table 5-14. Charging Nozzle Fatigue Usage Results (no OBE)	5-31
Table 5-15. RCS Hot Leg Surge Nozzle Detailed CUF Results for PATH6 (+OBE)	5-32
Table 5-16. RCS Hot Leg Surge Nozzle Detailed CUF Results for PATH7 (+OBE)	5-33
Table 5-17. RCS Hot Leg Surge Nozzle Detailed Fatigue Results for PATH6 (+OBE & S _m averaging)	5-34



Table 5-18. RCS Hot Leg Surge Nozzle Detailed CUF Results for PATH7 (+OBE & S_m averaging)	5-35
Table 5-19. EAF Factors (F_{en}) for RCS Hot Leg Surge Nozzle PATH6.....	5-37
Table 5-20. RCS Hot Leg Surge Nozzle EAF Results for Bounding PATH6	5-39

List of Figures

<u>Figure</u>	<u>Page</u>
Figure 4-1. Charging Nozzle Finite Element Model	4-2
Figure 4-2. Charging Nozzle Dimensions (as modeled).....	4-3
Figure 4-3. Assumed Worst Case Orientation for Bounding Run Piping Moments	4-12
Figure 4-4. Charging Nozzle Convection Surfaces	4-14
Figure 4-5. Charging Nozzle Mechanical Boundary Conditions	4-15
Figure 4-6. Charging Nozzle Coupled Boundary Conditions.....	4-16
Figure 4-7. Charging Nozzle Unit Internal Pressure Application	4-17
Figure 4-8. Charging Nozzle Full Finite Element Model.....	4-18
Figure 4-9. Charging Nozzle Stress Linearization PATH1	4-21
Figure 4-10. Charging Nozzle Stress Linearization PATH2 through PATH4	4-22
Figure 5-1. RCS Hot Leg Surge Nozzle Finite Element Model	5-2
Figure 5-2. RCS Hot Leg Surge Nozzle Dimensions (as modeled)	5-3
Figure 5-3. Typical I/O/stratification Transient.....	5-8
Figure 5-4. RCS Hot Leg Surge Nozzle Convection Surfaces	5-18
Figure 5-5. RCS Hot Leg Surge Nozzle Mechanical Boundary Conditions	5-19
Figure 5-6. RCS Hot Leg Surge Nozzle Unit Internal Pressure Application	5-20
Figure 5-7. RCS Hot Leg Surge Nozzle Full Finite Element Model.....	5-21
Figure 5-8. RCS Hot Leg Surge Nozzle Stress Linearization PATH1 and PATH2.....	5-23
Figure 5-9. RCS Hot Leg Surge Nozzle Stress Linearization PATH3 through PATH5	5-24
Figure 5-10. RCS Hot Leg Surge Nozzle Stress Linearization PATH6.....	5-25
Figure 5-11. RCS Hot Leg Surge Nozzle Stress Linearization PATH7.....	5-26

1.0 ACRONYMS

The following acronyms are used in this report.

3-D	Three-dimensional
ASME	American Society of Mechanical Engineers
CUF	Cumulative usage factor
DO	Dissolved oxygen
EAF	Environmentally-assisted fatigue
FEA	Finite element analysis
FSRF	Fatigue strength reduction factor
ID	Inside diameter
KPS	Kewaunee Power Station
MOP	Modified Operating Procedure
MRP	Materials Reliability Program (EPRI)
NRC	Nuclear Regulatory Commission
NSSS	Nuclear Steam Supply System
NUREG	Nuclear Regulatory Commission Regulation
OBE	Operating Basis Earthquake
OD	Outside diameter
PWR	Pressurized water reactor
PZR	Pressurizer
RCL	Reactor coolant loop
RCS	Reactor coolant system
RIS	Regulatory Information Summary
RTSR	Reload Transition Safety Report
SBF	Stress-based fatigue
SCF	Stress concentration factor
SI	Structural Integrity Associates, Inc.
SRSS	Square root sum of the squares
USAS	USA Standard
WOG	Westinghouse Owners Group
WSS	Westinghouse Systems Standard

2.0 BACKGROUND AND REPORT OBJECTIVE

KPS is currently submitting an application to the NRC in order to renew the license and extend operation to a period of 60 years. Plants are required to manage the aging effects of systems, structures and components in the scope of license renewal. Part 54 to Title 10 of the U.S. Code of Federal Regulations (10CFR54) specifies the “Requirements for Renewal of Operating Licenses for Nuclear Power Plants”.

NRC report NUREG-1801, the “Generic Aging Lessons Learned (GALL) Report” [4], identifies acceptable aging management programs, including programs for fatigue and cyclic operation. Although the NRC concluded that the effect of a reactor water environment is not a safety issue, the NRC does require of all license renewal applicants to assess the fatigue effect from a reactor water environment for the entire 60 year period of extended operation. High fatigue locations studied in NRC report NUREG/CR-6260 [2] are considered an appropriate sample for evaluation.

KPS demonstrated acceptable EAF for each NUREG/CR-6260 sample location during the course of initial license renewal activities. Two of these locations, the charging nozzle and the RCS hot leg surge nozzle, relied on EPRI’s FatiguePro software stress-based fatigue (SBF) monitoring results to demonstrate acceptability. FatiguePro SBF uses a simplified, single stress term methodology. Subsequent to these analyses, the NRC staff expressed concern about the use of simplified, single stress term methods of fatigue analysis of nuclear plant components in Regulatory Issue Summary RIS-2008-30 [3].

This report summarizes work performed that provides independent fatigue analyses of the charging and RCS hot leg surge nozzles. This work used NRC approved methodology to address all concerns expressed in RIS-2008-30.



3.0 ANALYSIS CRITERIA AND METHODOLOGY

3.1 ASME Code Fatigue Calculations

The KPS Class 1 piping, which includes the charging and hot leg surge branch nozzles, were designed according to the requirements of USAS B31.1-1967, which requires no explicit fatigue analysis. Later, in response to NRC Bulletin 88-11, the pressurizer surge line (including the hot leg surge nozzle) was analyzed to the 1986 Edition of the ASME Boiler and Pressure Vessel Code, Section III, Subarticle NB-3600 to address the effects of thermal stratification. For the purposes of license renewal the NRC does require that fatigue calculations of the NUREG/CR-6260 [2] sample locations be performed in accordance with the requirements of the ASME Code Section III, but also allows use of later Code Editions. Therefore, the 2001 Edition of the ASME Code with Addenda through 2003 [1], approved by the NRC per 10CFR50.55a, was used for the EAF analyses of the charging and hot leg surge nozzles.

Detailed 3-D finite element models were developed using ANSYS [8], which is NRC approved software and also verified under SI's nuclear QA program. ASME Code temperature-dependent material properties for Class 1 components were used in the Finite Element Analysis (FEA). Linear elastically computed stresses for the relevant design transients were computed. Thermal transient stresses were added to static stresses due to pressure and piping loads, which were scaled based on the magnitudes of the pressure and piping loads. Fatigue strength reduction factors (FSRFs) or stress concentration factors (SCFs) were applied, as appropriate, to the analysis sections. All six, unique components of the stress tensor are used throughout the calculations.

SI's VESLFAT software [5], which is verified per SI's nuclear QA program, was used to perform the fatigue usage calculations in accordance with the fatigue usage portion of Section III of the ASME Code [1], Subarticle NB-3200 (Design by Analysis). VESLFAT performs the analysis required by NB-3222.4(e) for Service Levels A and B conditions defined by the user. The program computes the stress intensity range based on the stress component ranges for all event pairs [1, NB-3216.2] and evaluates the stress ranges for primary plus secondary and primary plus secondary plus peak stress based upon the six unique components of the stress tensor (3 direct and 3 shear stresses), considering the possibility of varying principal stress



directions. Primary plus secondary stress intensity range (S_n) is calculated as [1, Figure NB-3222-1]:

$$S_n = P_L + P_b + P_e + Q, \text{ where}$$

P_L = primary local membrane stress intensity range

P_b = primary bending stress intensity range

P_e = secondary expansion stress intensity range

Q = secondary membrane plus bending stress intensity range

The Code allowable stress intensity, S_m , was specified as a function of temperature for each analysis section. The input maximum metal temperature for both states of a load set pair is used to determine S_m from the user-defined values. If S_n is greater than $3S_m$, then the total stress range is increased by the strain concentration factor K_e , as described in NB-3228.5 [1].

When more than one load set is defined for either of the event pair loadings, the stress differences are determined for all of the potential loadings, saving the maximum for the event pair, based on the pair producing the largest alternating total stress intensity (S_{alt}), including the effects of K_e . S_{alt} is calculated as:

$$S_{alt} = (K_e S_p / 2) (E_{curve} / E_{analysis}), \text{ where}$$

K_e = strain concentration factor

S_p = primary plus secondary plus peak (total) stress intensity range

E_{curve} = modulus of elasticity shown on applicable fatigue curve

$E_{analysis}$ = modulus of elasticity used in the analysis, conservatively taken as E at the input maximum metal temperature of the load set pair (E becomes lower with increasing temperature)

The principal stresses for the stress ranges are determined by solving for the roots of the cubic equation:

$$S^3 - (\sigma_x + \sigma_y + \sigma_z)S^2 + (\sigma_x \sigma_y + \sigma_y \sigma_z + \sigma_z \sigma_x - \tau_{xy}^2 - \tau_{xz}^2 - \tau_{yz}^2)S - (\sigma_x \sigma_y \sigma_z + 2 \tau_{xy} \tau_{xz} \tau_{yz} - \sigma_z \tau_{xy}^2 - \sigma_y \tau_{xz}^2 - \sigma_x \tau_{yz}^2) = 0$$

The stress intensities for the load set pairs are reordered in decreasing order of S_{alt} , including a correction for the ratio of modulus of elasticity (E) from the fatigue curve divided by E from the analysis. This allows a fatigue table to be created to eliminate the number of cycles available for



each of the events of an event pair, allowing determination of fatigue usage per NB-3222.4(e) [1]. For each load set pair in the fatigue table, the allowable number of cycles is determined using logarithmic interpolation based on S_{alt} , per ASME Code requirements.

Unless justified otherwise, transients that consist of multiple extreme stress conditions (local maximum, or peak, and local minimum, or valley) were split so that each significant, extreme condition is treated as a separate event. Intermediate peaks or valleys that produce obvious alternating stress intensities below the fatigue curve endurance limit are negligible and may therefore be filtered out (not split separately). If multiple peaks result from different principal stresses peaking at slightly different times due to the thermal response behavior of the location, then the peaks were determined to be simultaneous and were therefore grouped into a single event. Peaks and valleys in pressure vessels and piping are typically associated with upward and downward temperature or pressure ramps or abrupt changes in temperature slopes.

The cumulative effect of load set pairs is calculated using a linear damage relationship (Miner's Rule). That is:

$$CUF = \sum_{i=1}^k \frac{n_i}{N_i} \leq 1.0$$

where:	k	=	number of stress levels in the loading spectrum (i.e., the number of rows in the fatigue table)
	n_i	=	number of cycles at the i^{th} stress level, S_{ai}
	N_i	=	fatigue life at S_{ai}
	S_a	=	amplitude of the alternating stress intensity
	CUF	=	Cumulative usage factor

3.2 EAF Calculations

EAF calculations were performed for the reactor water environmental effects. The evaluation uses the appropriate F_{en} relationships from NUREG/CR-5704 [6] (for austenitic stainless steels), which is the relevant material at the analyzed sections of the charging and hot leg surge branch nozzles. MRP-47 Rev. 1 [7] was also used for guidance in the calculations. These expressions are:

For Types 304 and 316 Stainless Steel: $F_{en} = e^{0.935 - T^* \dot{\epsilon}^* O^*}$

where:

F_{en}	=	fatigue life correction factor
T	=	service temperature of transient, °C
T^*	=	0 for $T < 200^\circ\text{C}$
	=	1 for $T \geq 200^\circ\text{C}$
$\dot{\epsilon}^*$	=	0 for strain rate, $\dot{\epsilon} > 0.4\%/ \text{sec}$
	=	$\ln(\dot{\epsilon}/0.4)$ for $0.0004 \leq \dot{\epsilon} \leq 0.4\%/ \text{sec}$
	=	$\ln(0.0004/0.4)$ for $\dot{\epsilon} < 0.0004\%/ \text{sec}$
O^*	=	0.260 for dissolved oxygen, $\text{DO} < 0.05$ parts per million (ppm)
	=	0.172 for $\text{DO} \geq 0.05$ ppm

Using the above equation, resulting F_{en} values for several sets of parameters are shown below.

The bounding (maximum possible) F_{en} value for stainless steel material is 15.35.

$F_{en} = 2.55$ ($T < 200^\circ\text{C}$, any $\dot{\epsilon}$, any DO)
 $F_{en} = 2.55$ ($T \geq 200^\circ\text{C}$, $\dot{\epsilon} \geq 0.4\%/ \text{sec}$, any DO)
 $F_{en} = 3.78$ ($T \geq 200^\circ\text{C}$, $\dot{\epsilon} = 0.04\%/ \text{sec}$, $\text{DO} \geq 0.05$ ppm)
 $F_{en} = 4.64$ ($T \geq 200^\circ\text{C}$, $\dot{\epsilon} = 0.04\%/ \text{sec}$, $\text{DO} < 0.05$ ppm)
 $F_{en} = 5.62$ ($T \geq 200^\circ\text{C}$, $\dot{\epsilon} = 0.004\%/ \text{sec}$, $\text{DO} \geq 0.05$ ppm)
 $F_{en} = 8.43$ ($T \geq 200^\circ\text{C}$, $\dot{\epsilon} = 0.004\%/ \text{sec}$, $\text{DO} < 0.05$ ppm)
 $F_{en} = 8.36$ ($T \geq 200^\circ\text{C}$, $\dot{\epsilon} \leq 0.0004\%/ \text{sec}$, $\text{DO} \geq 0.05$ ppm)
 $F_{en} = 15.35$ ($T \geq 200^\circ\text{C}$, $\dot{\epsilon} \leq 0.0004\%/ \text{sec}$, $\text{DO} < 0.05$ ppm)

The fatigue usage contribution for each row in the fatigue tables was multiplied by either an F_{en} value specific to the load pair or a bounding value to account for the reduction in life due to the reactor water environment. In the F_{en} calculations for the two nozzles the DO content was assumed to be less than 0.05 ppm, which is a conservative assumption when using the F_{en} formulation above for stainless steel materials. Higher DO values at temperatures above 150°C (302°F) are not reasonably expected in a PWR light water environment. Where detailed strain rates were computed, the Integrated Strain Rate methodology, as described in the MRP-47, Rev. 1 [7] guidance document, was utilized.

4.0 CHARGING NOZZLE

4.1 Component Description and Finite Element Model

The austenitic stainless steel charging nozzle is a fitting welded to the Loop B RCS cold leg. A thermal sleeve is attached to the nozzle, and the charging piping is slip fitted into the nozzle with an OD socket weld. A 3-D finite element model was developed in the Reference 9 calculation package using the ANSYS software and is shown on Figure 4-1. As-modeled dimensions are shown on Figure 4-2.

Material designations for the various components used in the model are shown on Table 4-1. The water gap between the thermal sleeve and the nozzle and cold leg piping was modeled using an effective conductivity that accounts for free convection in an enclosed annulus. This effective conductivity was used to compute accurate temperature distributions throughout the component in the transient thermal analyses and was removed from the model during stress analyses.

Material properties are shown in Table 4-2, taken from the ASME Code, Section II Part D [1], with the exception of the water gap thermal properties, which were specified or calculated, as documented in Reference [9], and the density of the steel components, which was assumed to be 0.283 lb/in³.

Table 4-1. Charging Nozzle Material Designations

Component	Material
Cold Leg Piping	A351 GR CF8M
Charging Nozzle	A182 F304
Charging Nozzle Piping	A376 TP304
Thermal Sleeve	A312 TP316

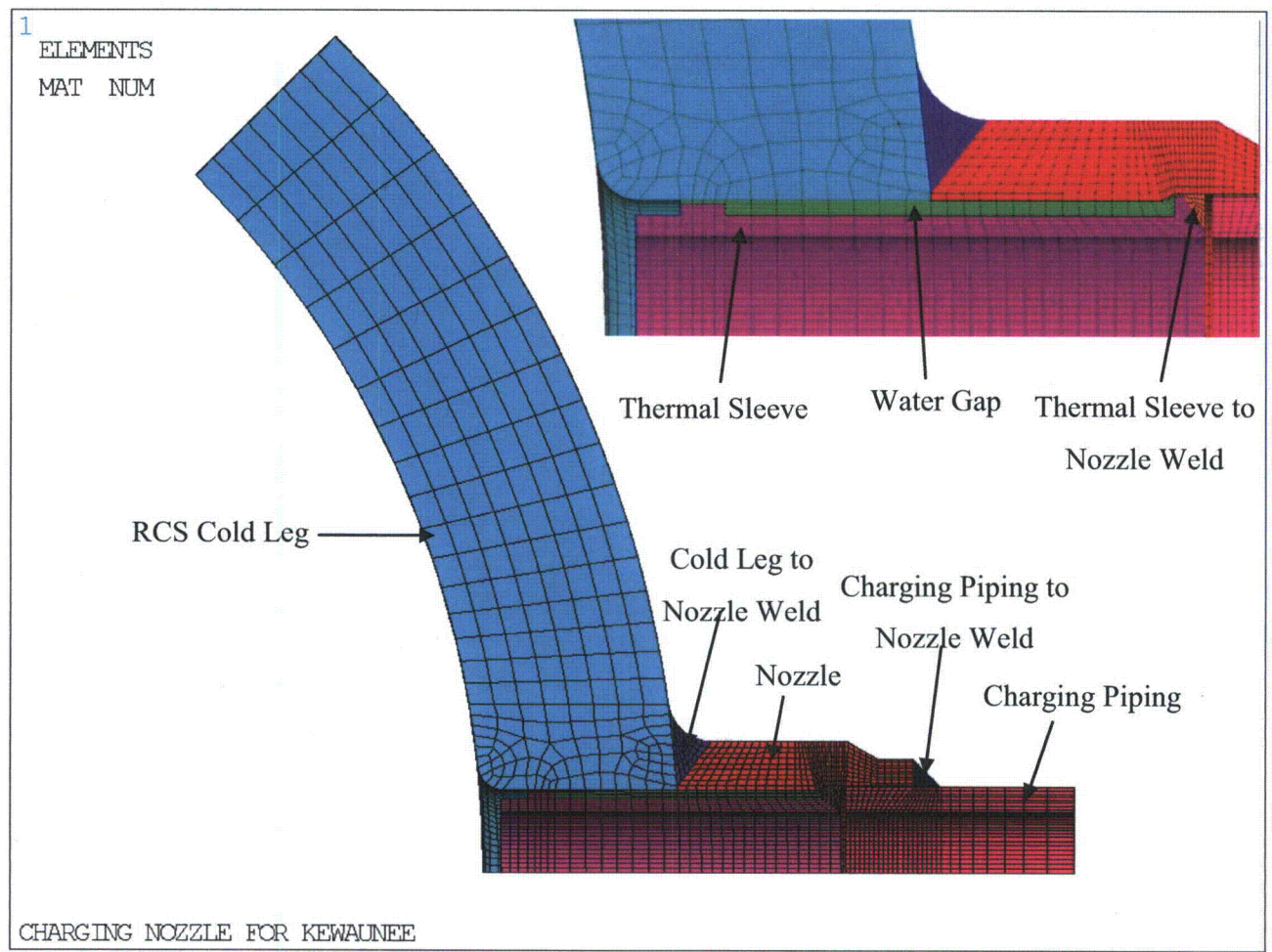


Figure 4-1. Charging Nozzle Finite Element Model

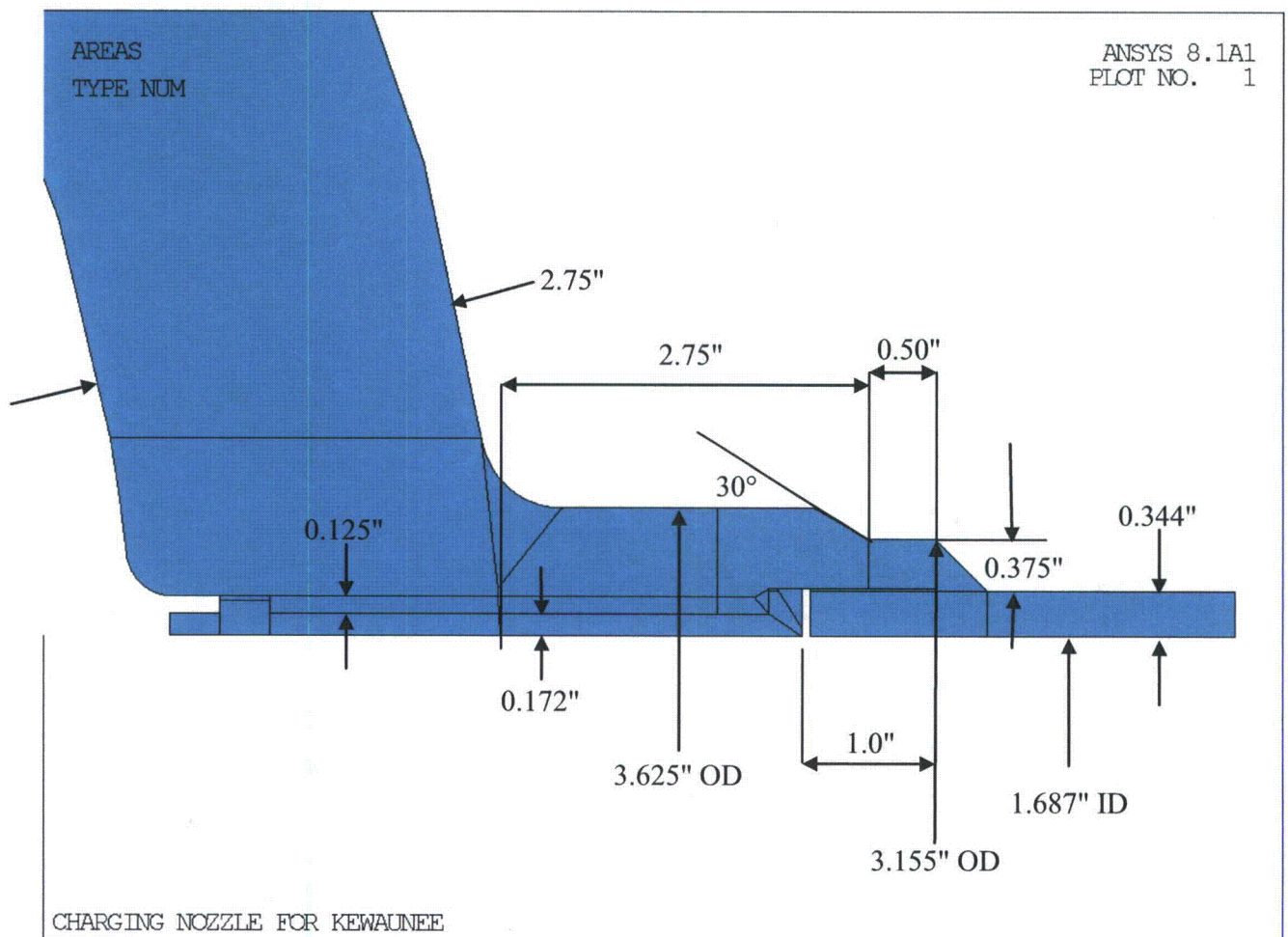


Figure 4-2. Charging Nozzle Dimensions (as modeled)

Table 4-2. Charging Nozzle Material Properties

Material No.	Description	Temperature (°F)	Young's Modulus, $E \times 10^6$ (psi)	Mean Coefficient of Thermal Expansion, $\alpha \times 10^{-6}$ (1/°F)	Conductivity, k (BTU/hr-ft-°F) (See Note 1)	Specific Heat, Cp (BTU/lbm-°F)	Density (lb/ft ³) (See Note 2)
1	A376 TP304 A182 F304 (18Cr-8Ni) Charging Piping Charging Nozzle	70	28.3	8.5	8.6	0.116	489.024
		100	28.1	8.6	8.7	0.117	
		150	27.9	8.8	9.0	0.120	
		200	27.6	8.9	9.3	0.122	
		250	27.3	9.1	9.6	0.124	
		300	27.0	9.2	9.8	0.125	
		350	26.8	9.3	10.1	0.127	
		400	26.5	9.5	10.4	0.129	
		450	26.2	9.6	10.6	0.130	
		500	25.8	9.7	10.9	0.131	
		550	25.6	9.8	11.1	0.132	
		600	25.3	9.8	11.3	0.133	
		650	25.1	9.9	11.6	0.134	
		700	24.8	10	11.8	0.135	
2	A351 GRCF8M A312 TP316 (16Cr-12Ni-2Mo) RCS Cold Leg Thermal Sleeve	70	28.3	8.5	8.2	0.121	489.024
		100	28.1	8.6	8.3	0.121	
		150	27.9	8.8	8.6	0.124	
		200	27.6	8.9	8.8	0.124	
		250	27.3	9.1	9.1	0.127	
		300	27.0	9.2	9.3	0.127	
		350	26.8	9.3	9.5	0.128	
		400	26.5	9.5	9.8	0.129	
		450	26.2	9.6	10	0.130	
		500	25.8	9.7	10.2	0.130	
		550	25.6	9.8	10.5	0.133	
		600	25.3	9.8	10.7	0.133	
		650	25.1	9.9	10.9	0.133	
		700	24.8	10	11.2	0.135	
3	Water Gap	70	N/A	N/A	4.1	0.999	62.25
		100				0.999	62.1
		150				1.0045	61.1
		200				1.01	60.1
		250				1.02	58.7
		300				1.03	57.3
		350				1.055	55.45
		400				1.08	53.6
		450				1.135	51.3
		500				1.19	49.0
		550				1.35	45.7
		600				1.51	42.4
		650				1.51	42.4
		700				1.51	42.4

Notes 1. Convert to BTU/sec-in-°F for input to ANSYS
2. Convert lb/ft³ to lb/in³ for input to ANSYS

4.2 Loading Definitions and Loading Combinations

4.2.1 Sources of Information for Design Transients

4.2.1.1 Transient Definitions

The charging nozzle was designed to USAS B31.1 requirements, which require no explicit fatigue analysis for the RCS and attached piping. Guidance in developing conservative, bounding transients was therefore taken from the Westinghouse Systems Standard (WSS). WSS 1.3.F [27] defines transients for the NSSS RCS and WSS 1.3.X [28] defines transients for the NSSS auxiliary equipment. Transients specific to two-loop Westinghouse PWR's, applicable to KPS, are provided in the WSS. The WSS transients include temperature, pressure and flow rate histories.

The approach taken here in selecting transients for the KPS charging nozzle is reasonable and consistent with that taken in NUREG/CR-6260 for the "Older Vintage Westinghouse Plant" charging nozzle. For example, Section 5.5.4 is quoted, in part, below:

"Since the piping was designed to the rules of B31.1 piping code, no fatigue analyses had been conducted. Consequently, the INEL staff performed a fatigue analysis using representative transients based on the charging nozzle analyses from the other PWR plants reviewed in this study..."

4.2.1.2 Effects of Power Uprate

KPS has initiated a 7.4% power uprating program. It was concluded that "the effects on the class 1 Auxiliary Piping systems that are attached to the RCL are insignificant due to the RTSR / 7.4% power uprating program" [11, p. 5]. Additionally, the range of design cold leg temperatures for the power uprate at full-load conditions is 521.9°F to 539.2°F [12, p. 3-7], which is considerably lower than the 560°F operating temperature assumed in WSS 1.3.X. Fatigue usage at the charging nozzle is driven mainly by the temperature differential induced by cold injection of flow through an initially hot charging nozzle (and returning to hot conditions). The actual thermal transients experienced by the charging nozzle would therefore be considerably less severe than those assumed by the WSS, since the temperatures differences are less. Therefore,



for the reasons stated above, the WSS transients were determined to be sufficiently conservative to account for both pre and post power uprate conditions.

4.2.2 Operating Parameters and System Transients Considered

Kewaunee is a two loop plant. The following parameters are specified in the WSS:

Normal charging flow ($Q_{\text{chrg}} = 100\%$) = 55 gpm

Normal cold leg temperature $T_{\text{cold}} = 560^{\circ}\text{F}$

Normal charging temperature = 500°F

Normal RCS flow per loop = 94,500 gpm

Table 4-3 lists the transients evaluated for 60 years of operation. Design Cycles were taken from the WSS 1.3.F and WSS 1.3.X. The numbers of design cycles for the transients from the WSS are either bounding or equal to the numbers of cycles in the KPS USAR. The KPS Metal Fatigue of the Reactor Coolant Pressure Boundary Aging Management Program [29] will ensure that actual cycle counts remain within the assumed number of Design Cycles, or appropriate actions will be taken.

Table 4-3. Charging Nozzle Transients

Transient	Design Cycles
<u>Auxiliary Transients</u>	
Charging and letdown flow shutoff and return to service	60
Letdown flow shutoff with prompt return to service	200
Letdown flow shutoff with delayed return to service	20
Charging flow shutoff with prompt return to service	20
Charging flow shutoff with delayed return to service	20
Charging flow step decrease and return to normal	24,000
Charging flow step increase and return to normal	24,000
Letdown flow step decrease and return to normal	2,000
Letdown flow step increase and return to normal	24,000
<u>Normal Condition RCS Transients</u>	
RCP startup and shutdown	*
Plant heatup and cooldown	200
Unit loading and unloading between 0 and 15 percent of full power	*
Unit loading and unloading at 5 percent of full power/minute	*
Reduced temperature return to power	*
Step load increase and decrease of 10 percent of full power	*
Large step load decrease with steam dump	200
Steady state fluctuations	*
Boron concentration equalization	*
Feedwater cycling	*
Refueling	80
Turbine roll test	20
Primary side leakage test	200
Secondary side leakage test	*
<u>Upset Condition RCS Transients</u>	
Loss of load	80
Loss of power	40
Partial loss of flow	80
Reactor trip A - with no inadvertent cooldown	230
Reactor trip B - with cooldown and no S.I.	160
Reactor trip C - with cooldown and S.I.	10
Inadvertent RCS depressurization - Umbrella Case	20
Inadvertent RCS depressurization - Inadvertent auxiliary spray	10
Control rod drop	*
Excessive feedwater flow	30
OBE	1,000
<u>Test Condition RCS Transients</u>	
Primary side hydrostatic test	10
Secondary side hydrostatic test	*
Tube leakage test	*

Note: * This transient is judged to produce negligible fatigue usage at the charging nozzle, based on small/slow changes in cold leg temperature.



4.2.3 Transient Lumping

To simplify thermal analysis, bounding RCS transients were chosen based on maximum cold leg temperature changes and ramp rates to “lump” transients together into a single, conservative set. The following transients were chosen.

- Plant heatup, plant cooldown, and inadvertent RCS depressurization were analyzed separately due to their large temperature or pressure changes.
- Excessive feedwater flow was chosen as the bounding RCS downward transient. This was shown to bound the following transients:
 - Large step load decrease with steam dump
 - Turbine roll test
 - Reactor trip A - with no inadvertent cooldown
 - Reactor trip B - with cooldown and no S.I.
 - Reactor trip C - with cooldown and S.I.
- Loss of load was chosen as the bounding upward RCS transient. This bounds the following transients:
 - Loss of power
 - Partial loss of flow
 - Reactor trip A - with no inadvertent cooldown (also a downward transient)

4.2.4 Heat Transfer Coefficients

Heat transfer coefficients were not provided in the WSS. Conservative values were calculated by SI based on the temperatures and flow rate histories. For the cold leg and charging piping and nozzle, the following equation was used for turbulent flow in tubes.

$$Nu = 0.023 Re^{0.8} Pr^{0.4}, \text{ where}$$



Nu = Nusselt number = hD/k
 Re = Reynolds number = VD/ν
 Pr = Prandtl number, non-dimensional
 h = heat transfer coefficient
 D = inside diameter, feet
 k = thermal conductivity
 V = velocity, ft/sec = $Q/(\pi D^2/4)$
 Q = volumetric flow rate
 ν = kinematic viscosity

For conditions where there is no charging flow, there is swirl penetration from the RCS cold leg such that forced convection equations are appropriate. Guidance was taken from the EPRI MRP document MRP-132 [13] and MRP-146S [14]. The Reynolds number is calculated based on swirl velocity, $\Omega(x)$, which is given by:

$$\Omega(x) = (2U/D)[\Omega_0 D/(2U)]/[1 + (x/D)/(L_\Omega/D)]^\beta, \text{ where}$$

$$\Omega_0 D/(2U) = 0.63(D/D_R)$$

$$L_\Omega/D = 3.2$$

$$\beta = 1.4$$

U = RCS flow velocity

D = branch inside diameter

D_R = RCS diameter

x = axial distance from the RCS inside surface

The equation simplifies to:

$$\Omega(x) = \Omega_0/[1 + (x/D)/(3.2)]^{1.4}, \text{ where}$$

$$\Omega_0 = 1.26U/D_R$$

The formulae for Reynolds number based on the swirl flow and heat transfer coefficient are as follows:

$$Re = \frac{1}{2} \frac{\Omega D^2}{\nu}$$

$$h = 0.023 Re^{0.8} Pr^{0.3} (k/D) \quad (\text{for } Re > 10,000)$$

Table 4-4 summarizes all heat transfer coefficients that will be applied for the thermal transient analysis of the nozzle.

Table 4-4. Summary of Charging Nozzle Heat Transfer Coefficients, Btu/hr-ft²-°F

Q_{chrg} %	Pipe/nozzle	Thermal sleeve	Cold leg
0%	359	517	7,054
50%	1,590	1,590	7,054
100%	2,769	2,769	7,054
150%	3,830	3,830	7,054
180%	4,432	4,432	7,054

4.2.5 Piping Interface Loads

4.2.5.1 Branch Piping

Bounding charging nozzle / branch piping interface loads due to thermal expansion and operating basis earthquake are shown in Table 4-5. The piping loads were transformed into the ANSYS coordinate system by the analysts. OBE loads in two different orientations are shown (X and Z). The OBE orientation that maximized the fatigue usage was determined by the fatigue analyst.

OBE was specified to have 20 occurrences with 50 cycles each, for a total of 1,000 cycles. OBE was conservatively assumed to occur simultaneously with any transient, up to the total number of OBE events.

Table 4-5. Charging Nozzle Branch Piping Interface Loads

Load Type	Forces (lbf)			Moments (ft-lbf)		
	F_x	F_y	F_z	M_x	M_y	M_z
THERMAL EXPANSION	18	29	0	-5	28	176
OBE X QUAKE	10	24	8	36	18	58
OBE Z QUAKE	7	22	13	64	23	38

Piping interface loads from thermal expansion were scaled based on the following factor, T_{FACTOR}.

$T_{\text{FACTOR}} = (T_{\text{chrg}} - 70) / (500 - 70)$, where

T_{chrg} = charging nozzle local temperature during transient, °F

4.2.5.2 Run Piping

Conservative run piping interface loads for thermal expansion and OBE loading conditions were developed [26]. These loads at the branch nozzle location were not specifically tabulated in the available design input. However, interface loads were available at other sections of the same runs of piping. Standard structural analysis methodologies were utilized to calculate bounding interface load values at the location of interest. SRSS values were computed and assumed to be applied in the worst case orientation, as shown on Figure 4-3, to maximize the fatigue usage for conservatism.

The KPS replacement steam generator project contained the latest piping analysis of record for the Reactor Coolant Loop (RCL). Piping interface loads for thermal expansion and seismic loading conditions were contained in this report and were calculated based on a piping model of the RCL. Seismic OBE values are one half the seismic SSE values.

The thermal expansion values for the cold leg were assumed to represent conditions going from a stress-free temperature of 70°F to a design basis temperature of 543.6°F. The SRSS thermal moment for the charging nozzle was calculated to be 2662.363 in-kip. Based on the temperature of the cold leg, TCOLD, the thermal run piping moment at the charging nozzle, Mchg_thm, may be calculated as:

$$M_{\text{chg_thm}} = (T_{\text{COLD}} - 70) / (543.6 - 70) \cdot 2662.363 \text{ in-kip}$$

The OBE run piping moment at the charging nozzle was calculated to be 909.499 in-kip, and can reverse direction in equal magnitude.

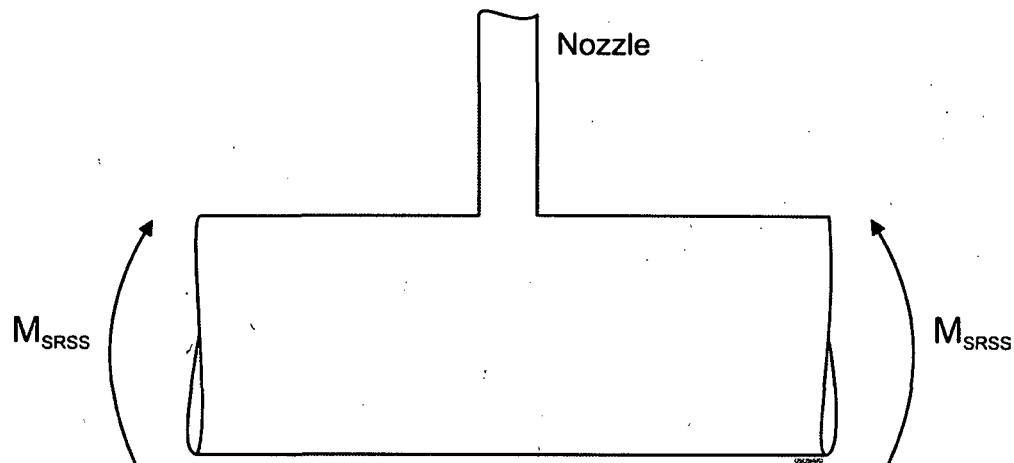


Figure 4-3. Assumed Worst Case Orientation for Bounding Run Piping Moments

4.3 Thermal and Mechanical Analyses

4.3.1 Methodology Overview

ANSYS [8] FEA was used to compute transient and static stresses [15] for input to the fatigue calculations. In computing transient (time-dependent) stresses a thermal analysis was first performed to compute temperature distributions throughout the model over time. The temperatures were then used to compute thermal stresses using standard, linear elastic FEA methodology. The following is a summary of the overall process used to perform the thermal and mechanical analyses.

- Apply bulk temperatures and heat transfer coefficients on defined convection surfaces to compute temperature distributions over time for all thermal transients.
- Perform stress analyses using temperature distribution results with the thermal sleeve (non-structural attachment) and water annulus (non-structural) removed.
- Perform stress analysis of unit internal pressure load case with thermal sleeve attachment and water annulus removed.
- Perform stress analyses of piping interface loads with thermal sleeve attachment and water annulus removed.

- Review stress results and select analysis sections (“paths”) along discontinuities and with high stress intensities.
- Extract linearized through-wall stresses at selected paths.

4.3.2 Boundary Conditions

4.3.2.1 Thermal Boundary Conditions

Due to symmetry, thermal transients were analyzed using a quarter model, as shown on Figure 4-1. Convection surfaces were defined in the loads calculation package [10] for the piping, thermal sleeve and RCS header regions. ANSYS macro files were created to apply temperature and film coefficients to the various convections surfaces, which are shown on Figure 4-4.

4.3.2.2 Mechanical Boundary Conditions

Symmetry and displacement boundary conditions were applied to the cut surfaces of the quarter model, as shown on Figure 4-5.

The edges of the charging piping and the cold leg piping were coupled in the axial (longitudinal) direction to prevent gross distortion of the cross sections and simulate the connected piping. The coupled conditions are shown on Figure 4-6.

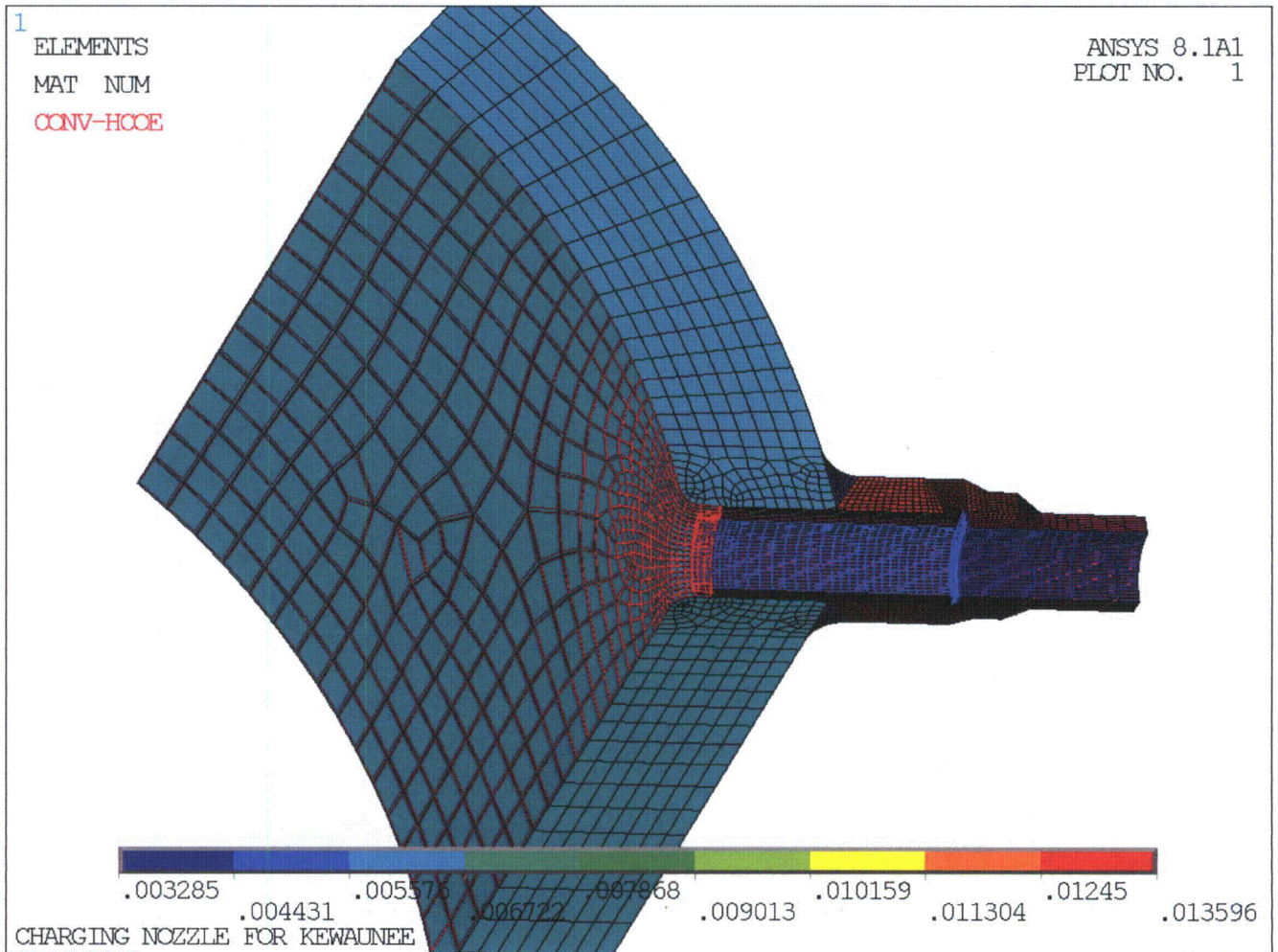


Figure 4-4. Charging Nozzle Convection Surfaces

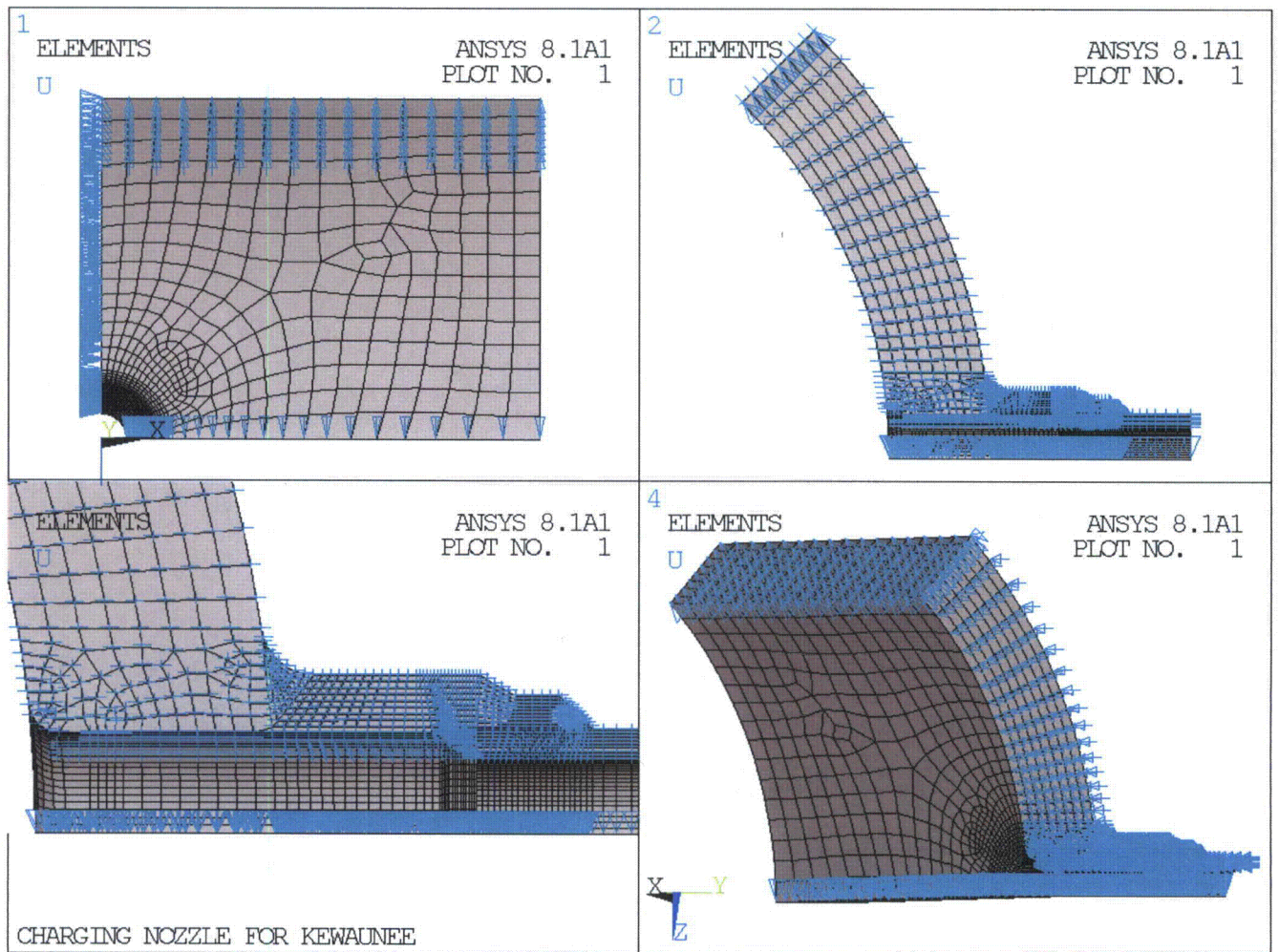


Figure 4-5. Charging Nozzle Mechanical Boundary Conditions

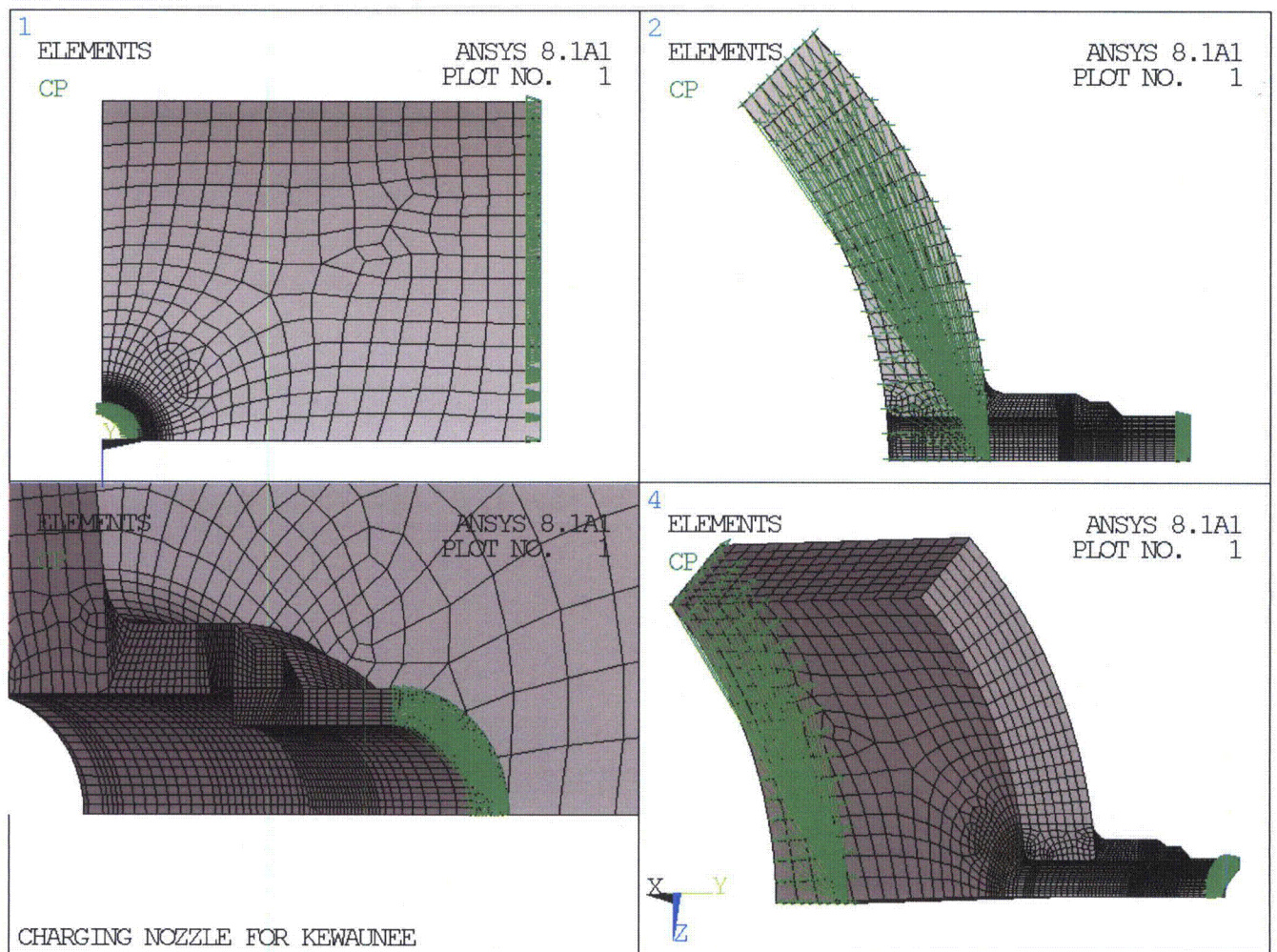


Figure 4-6. Charging Nozzle Coupled Boundary Conditions

4.3.3 Internal Pressure Analysis

A unit (1 psig) internal pressure analysis was performed so that results could be scaled to any internal pressure condition, based on linear elastic analysis. The pressure surfaces are shown in Figure 4-7. Cap loads were applied on the charging piping and the cold leg piping, based on multiplying the unit pressure by the ratio of the fluid cross sectional area to the metal cross sectional area. Values are negative to simulate tensile stress.

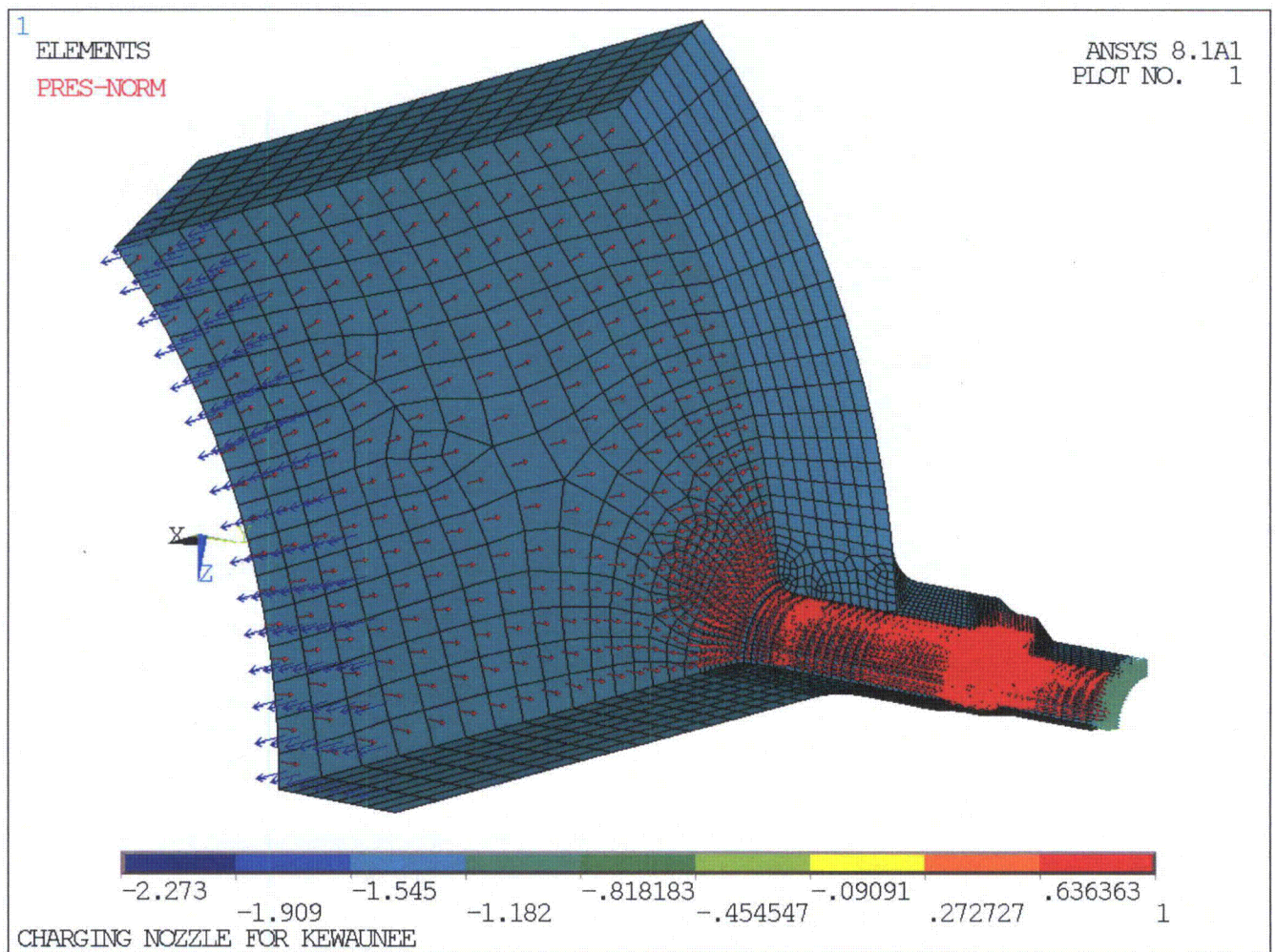


Figure 4-7. Charging Nozzle Unit Internal Pressure Application

4.3.4 Piping Interface Loading Analysis

4.3.4.1 Branch Piping

Table 4-5 lists branch piping interface loads for thermal and OBE conditions. For the stress analysis the loads were transformed into a coordinate system consistent with that of the FEA.

In order to apply these asymmetric loads, a full model was created from the quarter model using symmetry commands in ANSYS. The model is shown on Figure 4-8. A pilot node was created at the neutral axis of the charging piping along with a defined contact surface to apply the loads on the model.

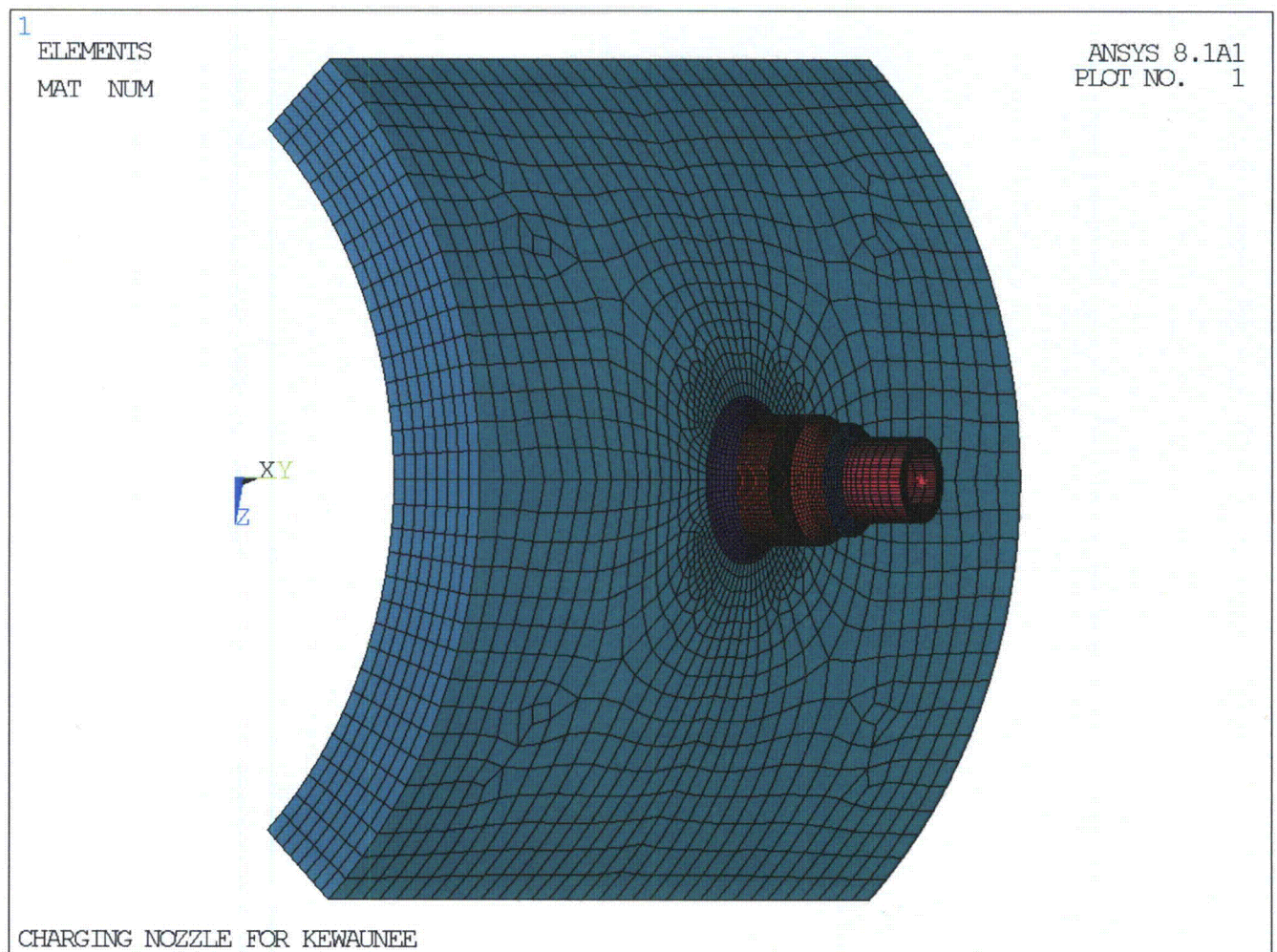


Figure 4-8. Charging Nozzle Full Finite Element Model

The boundary conditions were similar to the quarter model, except that the edge of the charging piping was not coupled in the circumferential direction in order to allow rotation of the pipe due to bending. The cut surfaces of cold leg piping had symmetry boundary conditions applied, the longitudinal direction of one edge of the cold leg piping had rollers applied, and the other side of the cold leg piping was coupled in the longitudinal direction to allow expansion but prevent gross distortion of the cross section to simulate the connected piping.

A benchmark analysis to verify proper application of the pilot node methodology was also conducted in [15] using a unit moment. The FEA computed axial stress was compared to that computed using a standard structural mechanics equation. The ANSYS results matched the hand calculation to within 3% and was considered to be more accurate, as it reflected the effects of gross structural discontinuities in the overall structure. Therefore the FEA methodology was confirmed to be appropriately executed.

4.3.4.2 Run Piping

A full model to analyze the cold leg run piping loads was created from the quarter model using symmetry commands in ANSYS. In addition, the cold leg piping portion of the model was extended 360° to allow an asymmetric load about the run pipe. A pilot node was then created on the neutral axis of the nozzle at the end of the cold leg piping along with a contact surface to apply moments on the model in the orientation specified on Figure 4-3. For mechanical boundary conditions, rollers were applied on one edge of the cold leg piping.

A unit moment was applied to the model. The unit moment may be scaled to any actual resultant moment based on cold leg temperature.

A two-part benchmark analysis to verify proper application of the pilot node methodology was also conducted in [15] using a unit moment. First, the FEA-computed axial stress was compared to that computed using a standard structural mechanics equation. The ANSYS result matched the hand calculation to within 0.6% and was considered to be more accurate, as it reflected the effects of gross structural discontinuities in the overall structure. Second, for the stress riser on the nozzle corner, guidance was taken from an NB-3600 equation (NB-3683.1(d)) to perform a benchmark of the computed stress. The maximum stress intensity computed by ANSYS was

approximately 8% higher than that calculated using the NB-3600 formula. The FEA calculations of the run pipe moment stresses therefore reasonably match the alternate benchmark calculations and are considered to be applied correctly.

4.3.5 Thermal Transients

The thermal stress analyses were performed by ANSYS using the temperature distributions computed in the thermal analyses for various time steps of each defined transient.

4.3.6 Selection of Analysis Sections (Paths)

Four stress linearization paths were chosen for fatigue analysis. PATH1 captures a high thermal stress intensity in the bore of the cold leg during Loss of Letdown transients. PATH2, PATH3, and PATH4 capture high stresses around the nozzle-to-charging piping weld and where FSRFs are required for the fatigue analysis due to the presence of the socket weld.

The paths for stress extraction are shown on Figure 4-9 and Figure 4-10. Because a full model was used for the analysis due to piping interface loads, the quarter model used for transient and pressure analysis will have different nodes. However, these represent the same physical location due to symmetry of the quarter model and because the stress results were extracted in a cylindrical coordinate system; that is, in this coordinate system radial, hoop and axial have consistent meanings around the cylinder circumference. The nodes for both the full and quarter models are shown on the figures.



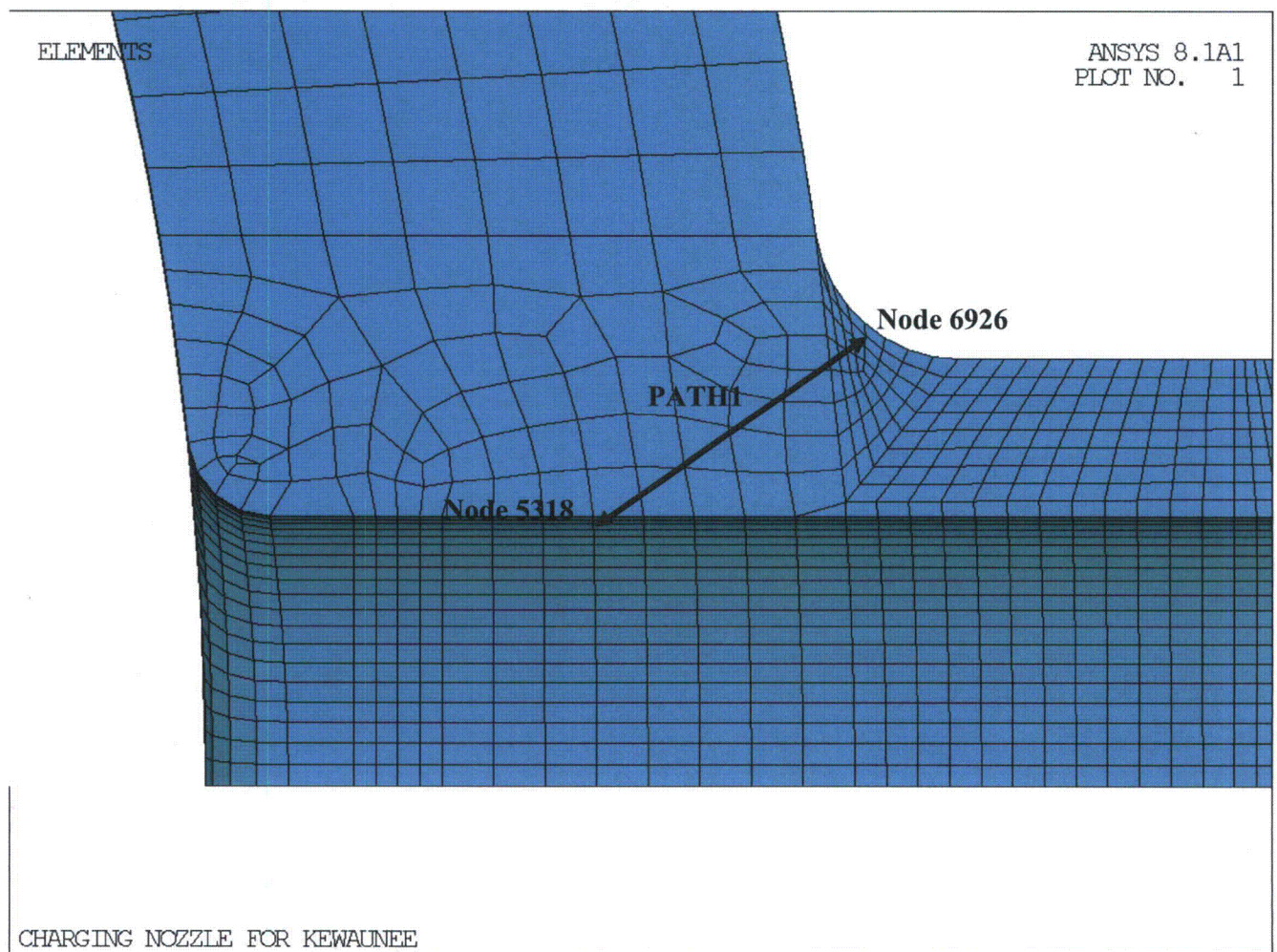
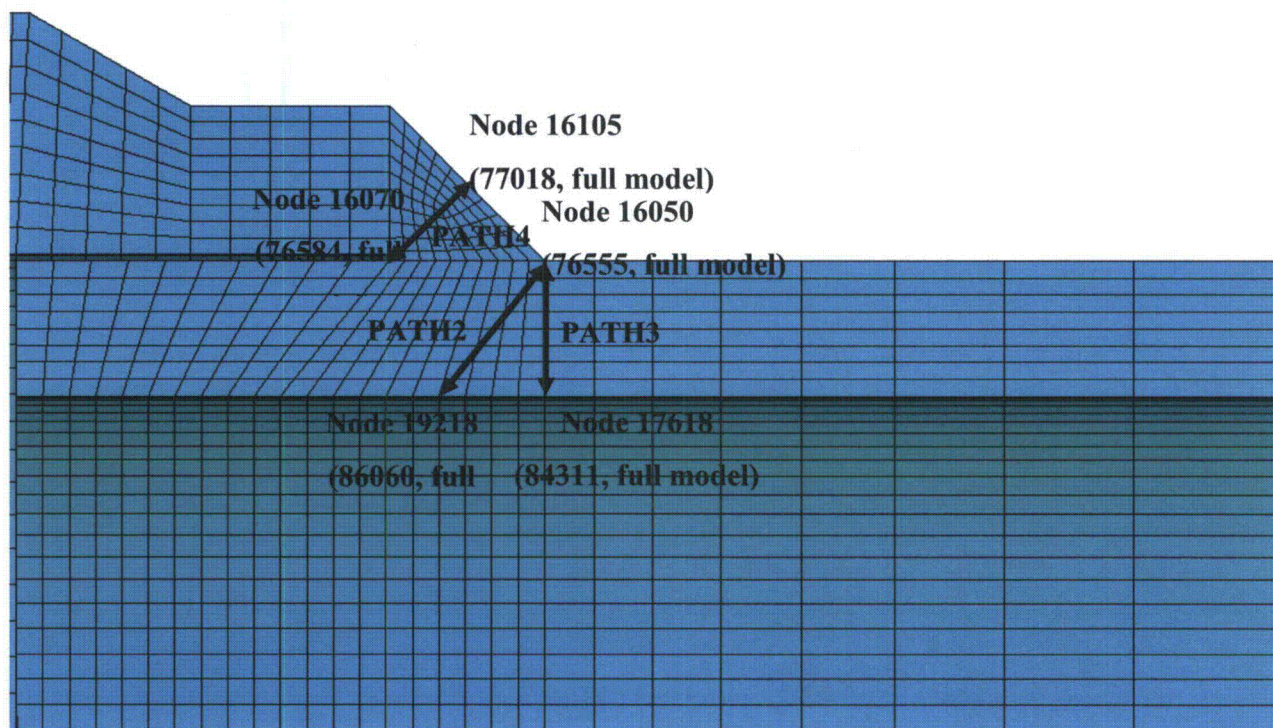


Figure 4-9. Charging Nozzle Stress Linearization PATH1



CHARGING NOZZLE FOR KEWAUNEE

Figure 4-10. Charging Nozzle Stress Linearization PATH2 through PATH4

Note: Actual nodes are rotated into the model to capture peak stresses.

4.3.7 Summary of FEA Analyses

Table 4-6 summarizes the various ANSYS thermal and mechanical analyses and post-processing operations performed to support the fatigue evaluation of the KPS charging nozzle.



Table 4-6. Summary of ANSYS Load Cases

Charging Nozzle Transients – Symmetric Loading on Quarter Model							
ANSYS							
#	Label	Description	Input Files		Output	Notes	
			Thermal	Stress	Post		
Charging/Letdown Shutoff Transients, As Analyzed							
1	TRAN1	Charging and letdown shutoff 1	TRAN1-T.INP	TRAN1-S.INP	LIN-STR-paths.INP	TRAN1-S#.LIN	
2	TRAN2	Charging and letdown shutoff 2	TRAN2-T.INP	TRAN2-S.INP	LIN-STR-paths.INP	TRAN2-S#.LIN	
3	TRAN3	Letdown shutoff, prompt return	TRAN3-T.INP	TRAN3-S.INP	LIN-STR-paths.INP	TRAN3-S#.LIN	
4	TRAN4	Letdown shutoff, delayed return 1	TRAN4-T.INP	TRAN4-S.INP	LIN-STR-paths.INP	TRAN4-S#.LIN	
5	TRAN5	Letdown shutoff, delayed return 2	-	-	-	-	
6	TRAN6	Charging shutoff, prompt return	TRAN6-T.INP	TRAN6-S.INP	LIN-STR-paths.INP	TRAN6-S#.LIN	
Charging/Letdown Flow Change Transients, As Analyzed							
7	TRAN7	Charging decrease and return	TRAN7-T.INP	TRAN7-S.INP	LIN-STR-paths.INP	TRAN7-S#.LIN	
8	TRAN8	Charging increase and return	TRAN8-T.INP	TRAN8-S.INP	LIN-STR-paths.INP	TRAN8-S#.LIN	
9	TRAN9	Letdown decrease and return 1	TRAN9-T.INP	TRAN9-S.INP	LIN-STR-paths.INP	TRAN9-S#.LIN	
10	TRAN10	Letdown decrease and return 2	TRAN10-T.INP	TRAN10-S.INP	LIN-STR-paths.INP	TRAN10-S#.LIN	
11	TRAN11	Letdown increase and return 1	TRAN11-T.INP	TRAN11-S.INP	LIN-STR-paths.INP	TRAN11-S#.LIN	
12	TRAN12	Letdown increase and return 2	TRAN12-T.INP	TRAN12-S.INP	LIN-STR-paths.INP	TRAN12-S#.LIN	
RCS Transients, As Analyzed							
13	TRAN13	Plant heatup	TRAN13-T.INP	TRAN13-S.INP	LIN-STR-paths.INP	TRAN13-S#.LIN	
14	TRAN14	Plant cooldown	TRAN14-T.INP	TRAN14-S.INP	LIN-STR-paths.INP	TRAN14-S#.LIN	
15	TRAN15	Refueling / zero load	-	-	-	-	
16	TRAN16	Primary leak test @ 2500 psia	-	-	-	-	
17	TRAN17	Loss of load	TRAN17-T.INP	TRAN17-S.INP	LIN-STR-paths.INP	TRAN17-S#.LIN	
18	TRAN18	Inadvertent RCS depress. / Inadvertent aux spray	TRAN18-T.INP	TRAN18-S.INP	LIN-STR-paths.INP	TRAN18-S#.LIN	
19	TRAN19	Excessive feedwater flow (modified)	TRAN19-T.INP	TRAN19-S.INP	LIN-STR-paths.INP	TRAN19-S#.LIN	
20	TRAN20	Primary hydro test @ 3122 psia	-	-	-	-	
Charging Nozzle Static Load Cases							
#	Label	Description	Stress		Post	Output	Notes
1	Thermal Exp.	Thermal Expansion Interface Loads	-	MOMENT.INP	LIN-STR-paths2.INP	MOMENT#.LIN	Analyzed at stress free, uniform temperature of 70°F on full FE model for all 4 load cases.
2	OBE X	OBE X Interface Loads	-	MOMENT.INP	LIN-STR-paths2.INP	MOMENT#.LIN	
3	OBE Z	OBE Z Interface Loads	-	MOMENT.INP	LIN-STR-paths2.INP	MOMENT#.LIN	
4	BENCHMARK	10,000 in-lbf X moment (benchmark)*	-	MOMENT.INP	LIN-STR-paths2.INP	MOMENT#.LIN	
5	RCS-MOM	RCS Unit Moment for scaling	-	RCS-MOM.INP	LIN-STR-RCS.INP	RCS-MOM-P1.LIN	
6	UNITPRESS	1 psig internal pressure	-	UNITPRESS.INP	LIN-STR-paths.INP	UNITPRESS#.LIN	

* = Used only to benchmark model to hand calculation

= PATH number from 1 through 4



4.4 ASME Code Fatigue Calculations

4.4.1 Fatigue Calculations

4.4.1.1 Stress Calculations

Fatigue calculations were performed in the Reference [16] calculation package using the methodology summarized in Section 3.1 of this report.

For PATH4, FSRFs were applied to the membrane plus bending (M+B) stress components. These FSRFs were conservatively applied to all six components (three normal, three shear) of the stress tensor. The following factors were chosen by taking guidance from the local stress indices (K indices) from NB-3600, as follows [1, Table NB-3681(a)-1]:

Pressure: 3.0
Moment: 2.0
Thermal: 3.0

In addition, for PATH4, the peak thermal stress components (PEAK) were added back into the total stress to capture the peak stress due to nonlinear radial temperature gradient, as required by Table NB-3217-2 of the ASME Code [1], as follows:

$$P+Q+F = (\text{ANSYS M+B})\text{FSRF} + (\text{ANSYS PEAK})$$

For the branch piping moments, the results were scaled based on temperature and applied in both the positive and negative direction to determine which direction maximizes the stresses at the location of interest.

4.4.1.2 Load Sets

Transients that consist of both stress peaks and valleys are split so that each successive peak or valley is treated as a separate load set. Table 4-7 shows the transients as input to VESLFAT. Since the Transient 5 (Letdown Shutoff, Delayed Return 2) temperature and pressure profile is identical to Transient 2 (Charging and Letdown Shutoff Return to Service 2), the 20 cycles from Transient 5 were added to the 80 cycles of Transient 2.



Table 4-7: Charging Nozzle Load Sets as Input to VESLFAT (PATH2)

Load Set	Transient	Start Time (sec.)*	Cycles
1	1. Charging and Letdown Shutoff 1	0	80
2	2. Charging and Letdown Shutoff 2	0	100**
3	2. Charging and Letdown Shutoff 2	30	100**
4	3. Letdown Shutoff, Prompt Return	0	200
5	3. Letdown Shutoff, Prompt Return	600	200
6	4. Letdown Shutoff, Delayed Return 1	0	20
7	4. Letdown Shutoff, Delayed Return 1	600	20
8	6. Charging Shutoff, Prompt Return	0	20
9	6. Charging Shutoff, Prompt Return	600	20
10	7. Charging Decrease and Return	0	24000
11	7. Charging Decrease and Return	1021	24000
12	8. Charging Increase and Return	0	24000
13	8. Charging Increase and Return	1022	24000
14	9. Letdown Decrease and Return 1	0	2000
15	9. Letdown Decrease and Return 1	600	2000
16	10. Letdown Decrease and Return 2	0	2000
17	11. Letdown Increase and Return 1	0	24000
18	11. Letdown Increase and Return 1	600	24000
19	12. Letdown Increase and Return 2	0	24000
20	12. Letdown Increase and Return 2	600	24000
21	13. Plant Heatup	0	200
22	14. Plant Cooldown	0	200
23	15. Refueling/Zero Load	0	290
24	16. Primary Leak Test @ 2500 psia	0	200
25	17. Loss of Load	0	430
26	17. Loss of Load	55	430
27	18. Inadvertent RCS Depressurization	0	30
28	18. Inadvertent RCS Depressurization	100	30
29	19. Excessive Feedwater Flow	0	650
30	19. Excessive Feedwater Flow	96	650
31	19. Excessive Feedwater Flow	491	650
32	20. Primary Hydro Test @ 3122 psia	0	10
33	Self-Cycling OBE	0	950
34	Tran + OBE***	0	50

* Note that stress peaks may occur after the start of the subsequent ramp.

** Note that 20 cycles of Letdown Shutoff, Delayed Return 2 are included.

*** Note that the numbers of cycles of the limiting transient are reduced by 50 cycles when OBE is applied. If the limiting transient has less than 50 cycles, 50 cycles is conservatively used and load set 34 is not necessary.



4.4.1.3 Material Properties

Table 4-8 lists the temperature-dependent material properties used in the analysis, and Table 4-9 lists the fatigue curve for stainless steel materials [1, Appendix I, Tables I-9.1 (Figure I-9.2.1) and I-9.2.2 (Curve C)]. At welds, the material that has lower S_m values is used. VESLFAT automatically scales the stresses by the ratio of E on the fatigue curve to E in the analysis, for purposes of determining allowable numbers of cycles, as required by the ASME Code.

Table 4-8. Charging Nozzle Material Properties for Fatigue Analysis

Material	T, °F	E, ksi	S_m , ksi
A351 Gr. CF8M (PATH1)	70	28300	20.0
	200	27600	20.0
	300	27000	20.0
	400	26500	19.2
	500	25800	17.9
	600	25300	17.0
	650	25050	16.6
	700	24800	16.3
A182 F304 and A376 TP304 (PATH2, 3, & 4)	70	28300	20.0
	200	27600	20.0
	300	27000	20.0
	400	26500	18.6
	500	25800	17.5
	600	25300	16.6
	650	25050	16.2
	700	24800	15.8

Table 4-9. Charging Nozzle Stainless Steel Fatigue Curve for Fatigue Analysis

Number of Cycles	S_n , ksi
10	708
20	512
50	345
100	261
200	201
500	148
1,000	119
2,000	97
5,000	76
10,000	64
20,000	55.5
50,000	46.3
100,000	40.8
200,000	35.9
500,000	31
1,000,000	28.2
2,000,000	22.8
5,000,000	18.4
10,000,000	16.4
20,000,000	15.2
50,000,000	14.3
100,000,000	14.1
1,000,000,000	13.9
10,000,000,000	13.7
100,000,000,000	13.6

4.4.1.4 Results

Initial fatigue calculations were made for all four selected paths, to determine the one with the highest CUF. Table 4-10 summarizes the initial fatigue usage results at the inside surface for PATHs 1 through 4.

Table 4-10. Charging Nozzle Fatigue Usage Results (no OBE)

Path	Load A	Bounding Load Set Pair		S_n , psi	K_e	S_{alt} , psi	Total Usage
		Load B					
1 Inside	4. Tran4	15. Tran13		44,921	1.000	26,625	0.0002
2 Inside	2. Tran2	4. Tran4		63,380	1.500	101,720	0.0300
3 Inside	2. Tran2	4. Tran4		26,017	1.000	77,914	0.0184
4 Inside	2. Tran2	4. Tran4		63,900	1.652	89,080	0.0190



PATH2 had the highest fatigue usage and was run with additional branch piping OBE loads. For these runs, moment stresses due to OBE were added to one of the thermal load sets in the pair with the highest alternating stress from the initial run. Table 4-11 shows the results.

Table 4-11. Charging Nozzle Detailed CUF Results for Bounding PATH2 (+OBE)

I	Load A	Load B	S_n	K_s	Salt	N	N_{allow}	U
1	7. Tran4	34. LS2+OBE	63447	1.504	101971	20	1688.25	0.0118
2	5. Tran3	34. LS2+OBE	58821	1.202	75812	30	5050.17	0.0059
3	2. Tran2	5. Tran3	58752	1.198	75573	50	5115.06	0.0098
4	5. Tran3	6. Tran4	43218	1	39434	20	120259	0.0002
5	4. Tran3	5. Tran3	43218	1	39434	100	120259	0.0008
6	4. Tran3	20. Tran12	29078	1	28808	100	855507	0.0001
7	9. Tran6	20. Tran12	21677	1	17686	20	6345700	0.0000
8	18. Tran11	20. Tran12	20522	1	15586	23880	1.59E+07	0.0015
9	15. Tran9	18. Tran11	17942	1	13652	120	3.03E+10	0.0000
Total Usage=								0.0302

4.4.2 EAF Calculations

The CUF for the KPS charging nozzle, without environmental effects, as calculated in the fatigue analysis is 0.0302. When multiplied by the maximum F_{en} of 15.35, the resulting EAF is 0.4636, which is below the allowable limit of 1.0. The KPS charging nozzle EAF is therefore acceptable for the period of extended operation if plant cycle counts remain within the limits presented in Table 4-3.

5.0 RCS HOT LEG SURGE NOZZLE

5.1 Component Description and Finite Element Model

The austenitic stainless steel RCS hot leg surge nozzle is a forging welded to the Loop B RCS hot leg. A non-structural thermal sleeve is attached to the nozzle, which is connected to the 10" schedule 140 surge line by a field butt weld. A 3-D finite element model was developed in the Reference [17] calculation package using the ANSYS software and is shown on Figure 5-1. As-modeled dimensions are shown on Figure 5-2.

Material designations for the various components used in the model are shown on Table 5-1.

The water gap between the thermal sleeve and the nozzle and hot leg piping was modeled using an effective conductivity that accounts for free convection in an enclosed annulus. This effective conductivity was used to compute accurate temperature distributions throughout the component in the transient thermal analyses and was removed from the model during stress analyses.

Material properties are shown on Table 5-2, taken from the ASME Code, Section II Part D [1], with the exception of the water gap thermal properties, which were specified or calculated, as documented in [17], and the density of the steel components, which was assumed to be 0.283 lb/in³.

Table 5-1. RCS Hot Leg Surge Nozzle Material Designations

Component	Material
Hot Leg	A-351 CF8M
Surge Nozzle	A-182 F316
Surge Piping	A376 TP316
Thermal Sleeve	A240 TP304

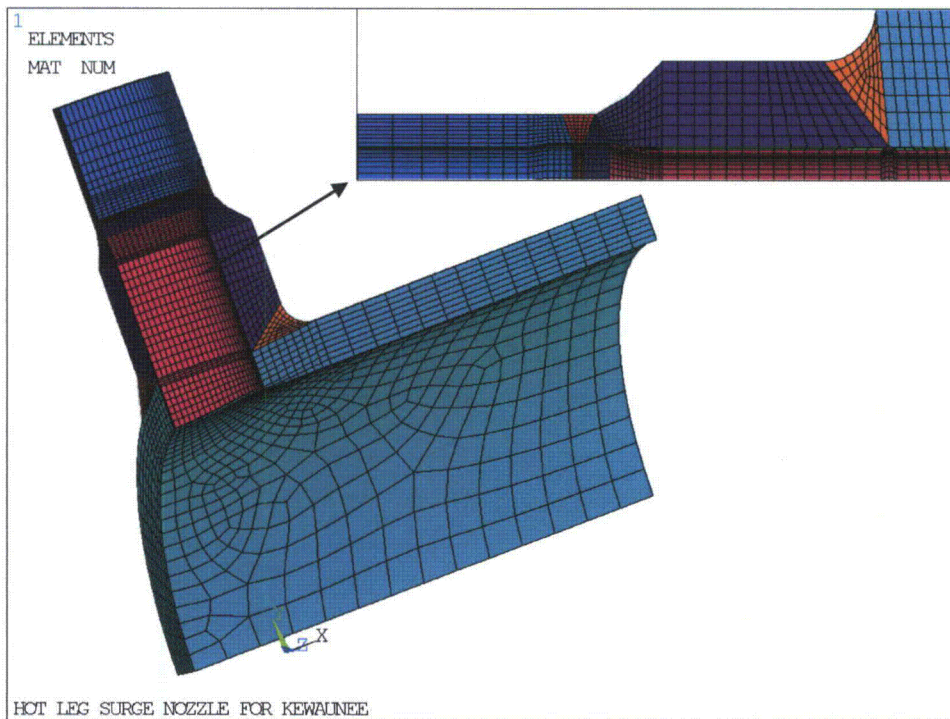
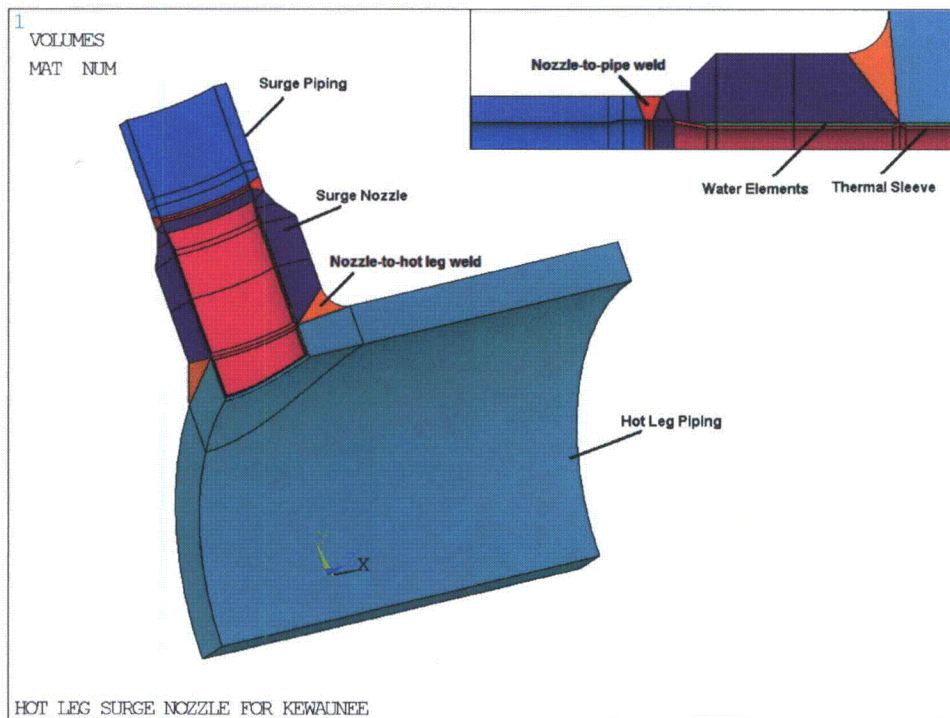


Figure 5-1. RCS Hot Leg Surge Nozzle Finite Element Model

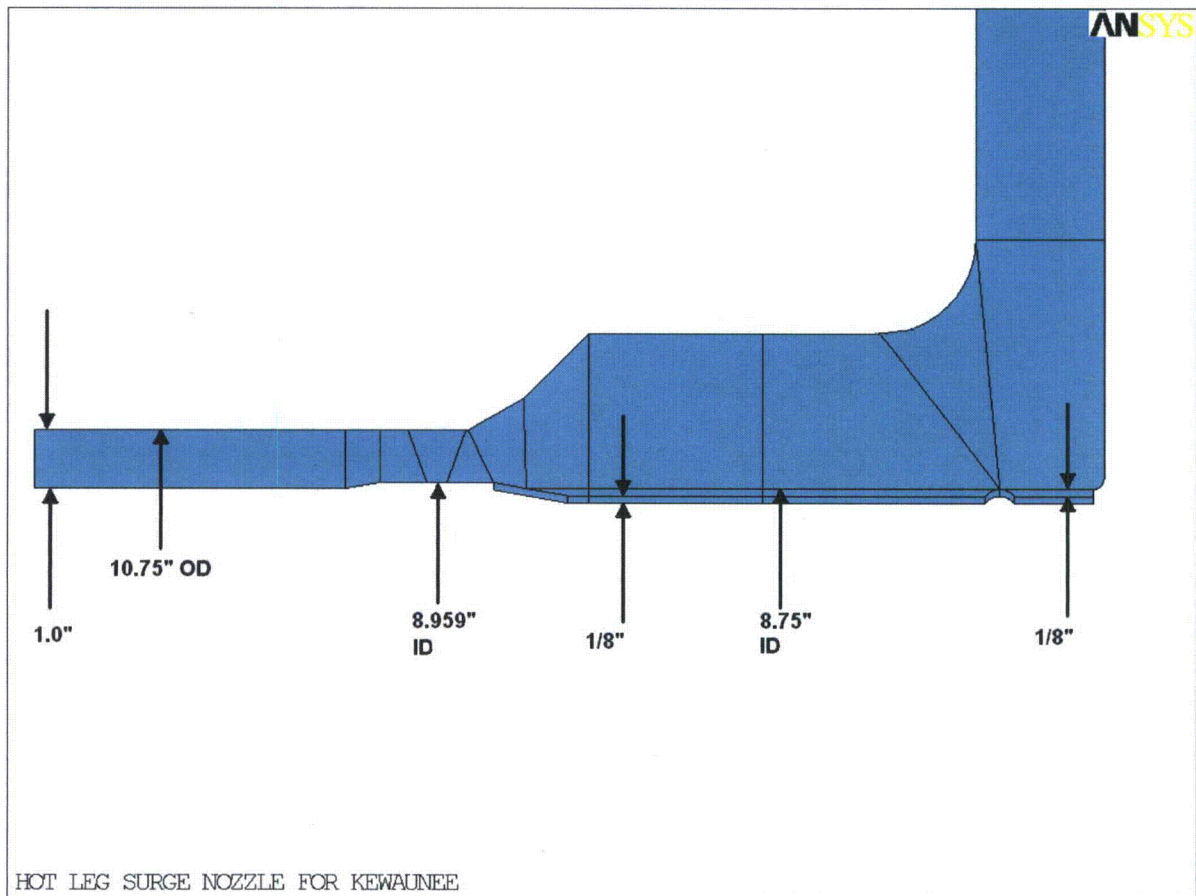


Figure 5-2. RCS Hot Leg Surge Nozzle Dimensions (as modeled)

Table 5-2. RCS Hot Leg Surge Nozzle Material Properties

Serial No.	Description	Temperature (°F)	Young's Modulus, E x 10 ⁶ (psi)	Mean Coefficient of Thermal Expansion, α x 10 ⁻⁶ (1/°F)	Conductivity, k (BTU/hr-ft-°F) (See Note 1)	Diffusivity, d (ft ² /hr)	Specific Heat, Cp (BTU/lbm-°F)	Density (lb/ft ³) (See Note 2)
1	SA376 TP316 (16Cr-12Ni-2Mo) (see note 3)	70	28.3	8.5	8.2	0.139	0.121	489.024
		100	28.1	8.6	8.3	0.140	0.121	
		150	27.9	8.8	8.6	0.142	0.124	
		200	27.6	8.9	8.8	0.145	0.124	
		250	27.3	9.1	9.1	0.147	0.127	
		300	27.0	9.2	9.3	0.150	0.127	
		350	26.8	9.3	9.5	0.152	0.128	
		400	26.5	9.5	9.8	0.155	0.129	
		450	26.2	9.6	10	0.157	0.130	
		500	25.8	9.7	10.2	0.160	0.130	
		550	25.6	9.8	10.5	0.162	0.133	
		600	25.3	9.8	10.7	0.165	0.133	
		650	25.1	9.9	10.9	0.167	0.133	
		700	24.8	10	11.2	0.170	0.135	
2	Water Gap	70	--	--	3.713	--	0.999	62.25
		100					0.999	62.1
		150					1.0045	61.1
		200					1.01	60.1
		250					1.02	58.7
		300					1.03	57.3
		350					1.055	55.45
		400					1.08	53.6
		450					1.135	51.3
		500					1.19	49.0
		550					1.35	45.7
		600					1.51	42.4
		650					1.51	42.4
		700					1.51	42.4



Table 5-2. RCS Hot Leg Surge Nozzle Material Properties (continued)

Serial No.	Description	Temperature (°F)	Young's Modulus, E x 10 ⁶ (psi)	Mean Coefficient of Thermal Expansion, α x 10 ⁻⁶ (1/°F)	Conductivity, k (BTU/hr-ft-°F) (See Note 1)	Diffusivity, d (ft ² /hr)	Specific Heat, Cp (BTU/lbm-°F)	Density (lb/ft ³) (See Note 2)
3	SA240 TP304 (18Cr-8Ni)	70	28.3	8.5	8.6	0.151	0.116	489.024
		100	28.1	8.6	8.7	0.152	0.117	
		150	27.9	8.8	9	0.154	0.120	
		200	27.6	8.9	9.3	0.156	0.122	
		250	27.3	9.1	9.6	0.158	0.124	
		300	27.0	9.2	9.8	0.160	0.125	
		350	26.8	9.3	10.1	0.162	0.127	
		400	26.5	9.5	10.4	0.165	0.129	
		450	26.2	9.6	10.6	0.167	0.130	
		500	25.8	9.7	10.9	0.170	0.131	
		550	25.6	9.8	11.1	0.172	0.132	
		600	25.3	9.8	11.3	0.174	0.133	
		650	25.1	9.9	11.6	0.177	0.134	
		700	24.8	10	11.8	0.179	0.135	

- Notes 1. Convert to BTU/sec-in-°F for input to ANSYS
2. Convert lb/ft³ to lb/in³ for input to ANSYS
3. Also includes the material properties of A-351 CF8M and A-182 F316 due to similar composition.

5.2 Loading Definitions and Loading Combinations

5.2.1 Sources of Information for Design Transients

5.2.1.1 Transient Definitions

The RCS hot leg surge nozzle was designed to USAS B31.1 requirements, which require no explicit fatigue analysis for the RCS and attached piping. Later, in response to NRC Bulletin 88-11, the pressurizer surge line (including the hot leg surge nozzle) was analyzed to ASME Section III, Subarticle NB-3600 to address the effects of thermal stratification. Guidance in developing conservative, bounding transients was taken from a combination of the following sources.



- RCS design transients were taken from the WSS 1.3.F. Transients specific to two-loop Westinghouse PWR's, applicable to KPS, are provided in the WSS. The WSS transients include temperature, pressure and flow rate histories.
- Insurge/outsurge (I/O) and stratification transients were developed based on the evaluation performed by Westinghouse [18] in response to NRC Bulletin 88-11 and an evaluation performed by the WOG in response to PZR insurge/outsurge [19]. The former evaluation collected thermocouple data specific to KPS operation at the time and a spectrum of I/O and stratification transients to bound plant operation, consisting of transients at several ΔT thresholds. The latter evaluated insurge/outsurge for several different modes of operation, including water solid, steam bubble, etc.

This analysis was conducted in two phases. In the first phase the "modified steam bubble" method of Heatup and Cooldown operation along with design numbers of cycles was conservatively assumed for the life of the plant. The second phase refined the analysis to credit the implementation in March 2006 of a Modified Operating Procedure (MOP), which was the "water solid" method of Heatup and Cooldown operation, along with cycles projected to 60 years based on rates of accumulation of past events.

5.2.1.2 Effects of Power Uprate

KPS has initiated a 7.4% power uprating program. It was concluded that "the effects on the RCL Branch Nozzles are insignificant due to the RTSR / 7.4% power uprating program" [11, p. 5].

5.2.2 Operating Parameters and System Transients Considered

Kewaunee is a two-loop plant. The following parameters are specified in the WSS:

- Full power HL temperature (T_{HL}) = 616.1°F
- Zero load HL temperature (T_{HL}) = 557°F
- Normal RCS pressure (P) = 2332 psia (bounding value) (This includes the head at the bottom of the RPV. It is conservative for the rest of the RCS)
- Thermal Design Flow (Q_{RCS}) = 94,500 gpm/loop
- Pressurizer temperature (T_{PZR}) = 653°F
- Pressurizer surge rate (Q_{SL}) = 11,695 gpm



The Q_{RCS} and Q_{SL} values shown above are nominal values used to scale the Q_{RCS} and Q_{SL} ratios in the transient tables.

Table 5-3 lists the RCS transients evaluated. 60-year projected cycles are based on monitoring results projected into the future, based on rates of accumulation of the past events.

I/O/stratification transients were evaluated with a template, simplified as follows.

- Initially there is stratification equal to ΔT_{strat} .
- During insurge, the top temperature in the piping ramps down to T_{RCS} , causing stratification to ramp down to zero.
- Once the insurge stops, stratification slowly reestablishes.
- After an indefinite period of time, outsurge occurs, such that the bottom temperature in the piping ramps up to T_{PZR} , causing stratification to ramp down to zero.
- Once the outsurge stops, stratification slowly reestablishes in the piping.

Figure 5-3 presents a typical PZR I/O transient. To simplify analysis, the above transient description is split into insurge and outsurge.

Table 5-4 lists the I/O/stratification transients evaluated for the pre-MOP period. Since the numbers of pre-MOP I/O transients are based on 58 Heatups and 58 Cooldowns, and there are 110 projected Heatups and Cooldowns for 60 years, the estimated number of post-MOP Heatups and Cooldowns is:

$$110 - 58 = 52 \text{ Heatups and } 52 \text{ Cooldowns}$$

Using this information and the distribution of cycles for the water solid methods [19, Table 4-13], the post-MOP PZR I/O transient spectrum is determined as shown in Table 5-5. Pressurizer temperature (T_{PZR}) is 440°F for Heatup [19, Figure 2-5] and 451°F for Cooldown [19, Figure 2-6], and RCS temperature T_{RCS} was calculated as $T_{PZR} - \Delta T$. To simplify the analysis, the surges are grouped as shown in Table 5-6.

For transients that have experienced zero events to-date, at least one event is postulated for future operation for conservatism. The KPS Metal Fatigue of the Reactor Coolant Pressure Boundary Aging Management Program [29] will ensure that actual cycle counts remain within the assumed number of analyzed, or appropriate actions will be taken.

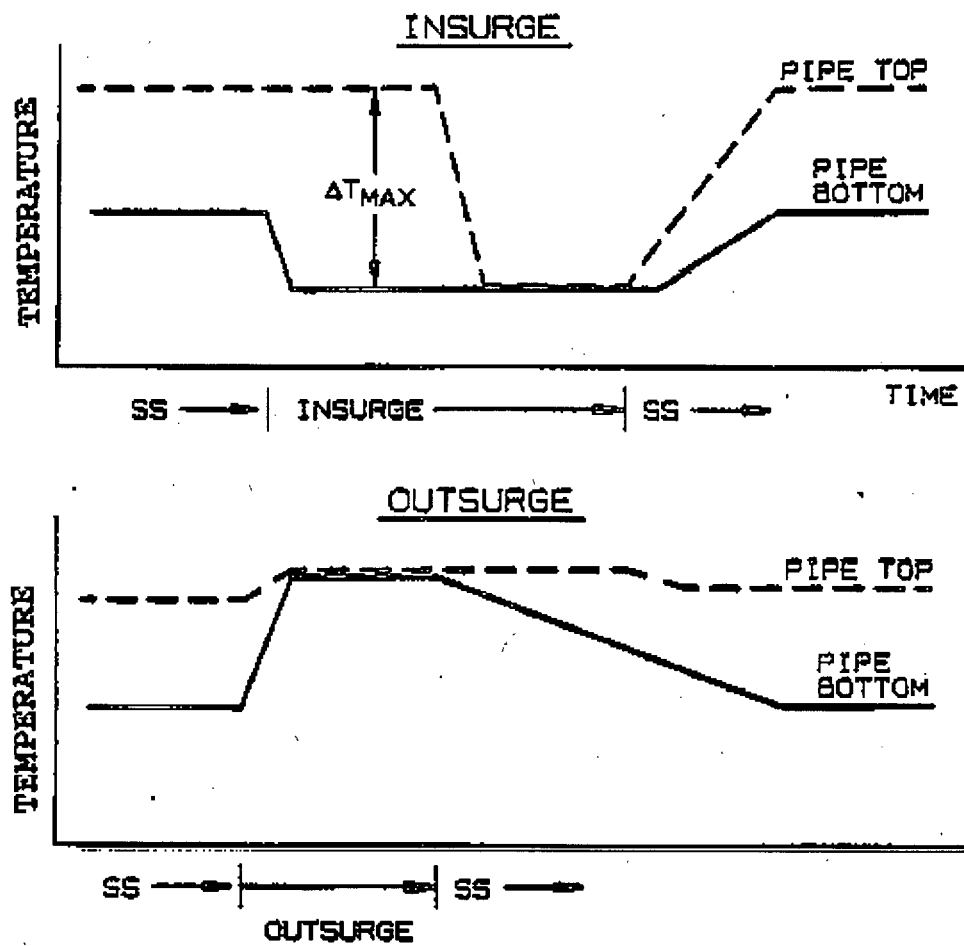


Figure 5-3. Typical I/O/stratification Transient

Table 5-3. RCS Transients for Hot Leg Surge Nozzle

Condition	Plant Event	60-Year Projected Cycles
Normal	RCP startup and shutdown	*
	RCS Heatup	110
	RCS Cooldown	108
	Unit loading/unloading between 0 and 15% of full power	*
	Plant Loading at 5% Power/Minute	214
	Plant Unloading at 5% Power/Minute	150
	Reduced temperature return to power	*
	Step Load Increase of 10% Power	*
	Step Load Decrease of 10% Power	*
	Large Step Load Decrease (with steam dump)	14
	Steady state fluctuations	*
	Boron concentration equalization	*
	Feedwater cycling	*
	Refueling	37***
Upset	Loss of Load	0
	Loss of Power	4
	Partial Loss of Flow	0
	Reactor Trip at Power with No Cooldown (A)	114
	Reactor Trip with Cooldown and No SI (B)	****
	Reactor Trip with Cooldown and SI (C)	****
	Inadvertent RCS Depressurization	0***
	Inadvertent Auxiliary Spray Actuation	0***
	Control rod drop	80**
	Excessive feedwater flow	30**
Test	Operating Basis Earthquake	0***
	Turbine Roll Test	2
	Primary Side Leak Test	48
	Primary Side Hydrostatic Test	2

* This transient is judged to be negligible.

** From the surge line stratification analysis [18].

*** From cycle projections performed by SI [20, Table 9].

**** Included with Reactor Trip A.



Table 5-4. I/O/stratification Cycles for Pre-MOP Period

Label	Cycles		ΔT_{strat} , °F	T_{PZR_2} , °F	T_{RCS_2} , °F
	per 200 HC	per 58 HC			
Exceedance	2	0.6	334	455	140
Exceedance	2	0.6	331	455	140
Exceedance	4	1.2	321	455	140
HC1	60	17.4	304	455	140
HC2	105	30.5	285	455	140
HC3	108	31.3	275	455	140
HC4	27	7.8	250	455	140
HC5	225	65.3	200	455	140
HC6	273	79.2	175	455	140
HC7	2202	638.6	150	455	140
HC9	1200	348.0	150	653	550

Table 5-5. I/O/stratification Cycles for Post-MOP Period

	% of Total	Cycles	ΔT , °F	T_{PZR_2} , °F	T_{RCS_2} , °F
Heatup	21%	21.8	210	440	230
	34%	35.4	197	440	243
	36%	37.4	177	440	263
	9%	9.4	164	440	276
Cooldown	14%	14.6	210	451	241
	33%	34.3	197	451	254
	33%	34.3	177	451	274
	20%	20.8	164	451	287
Grouped		106.1	210	451	241
		101.9	177	451	274



Table 5-6. Summary of All I/O/stratification Transients

Type	Transient	Cycles	ΔT_{strat} , °F	T_{PZR} , °F	T_{RCS} , °F
Pre-MOP	PIO334	1	334	455	140
	PIO331	1	331	455	140
	PIO321	2	321	455	140
	PIO304	18	304	455	140
	PIO285	31	285	455	140
	PIO275	32	275	455	140
	PIO250	8	250	455	140
	PIO200	66	200	455	140
	PIO175	80	175	455	140
	PIO150	639	150	455	140
	PIO150H	348	150	653	550
Post-MOP	PIO210	107	210	451	241
	PIO177	102	177	451	274

5.2.3 Transient Lumping

To simplify the fatigue usage analysis, selected RCS transients were grouped based on nozzle temperature, temperature ramp rate, and pressure. The bounding transient has nozzle temperature range, ramp rates, and pressure maximum and minimum values that bound all transients in the group.

The following transients were analyzed separately due to large temperature or pressure changes, or rapid temperature change:

- Plant Heatup
- Plant Cooldown
- Inadvertent RCS depressurization/inadvertent auxiliary spray
- Primary leak test
- Primary hydro test
- Refueling

The following transients, although not severe, are analyzed separately due to the large numbers of cycles:

- Plant loading 5%/minute
- Plant unloading 5%/minute



The following transients all begin with a sharp temperature rise, followed by a moderate to rapid cooldown, accompanied in most cases by a significant pressure drop.

- Large step load decrease
- Loss of load
- Loss of power
- Partial loss of flow
- Reactor trip A
- Reactor trip B
- Reactor trip C
- Control rod drop
- Excessive feedwater flow
- Turbine roll test

A bounding transient was constructed by combining loss of load, excessive feedwater flow, and turbine roll test.

A summary of all transients that were analyzed after lumping and adjusting numbers of cycles for conservatism is shown on Table 5-7.



Table 5-7. Summary of All RCS Hot Leg Surge Nozzle Transients to be Analyzed

Event	Cycles
RCS Heatup	110**
RCS Cooldown	110**
Plant Loading at 5% Power/Minute	214
Plant Unloading at 5% Power/Minute	150
RCS Group	244
Inadvertent RCS Depress./Aux Spray	1****
Refueling	87***
Primary Side Leak Test	48
Primary Side Hydrostatic Test	2
Operating Basis Earthquake	1****
PIO334	1
PIO331	1
PIO321	2
PIO304	18
PIO285	31
PIO275	32
PIO250	8
PIO200	66
PIO175	80
PIO150	639
PIO150H	348
PIO210	107
PIO177	102

** Bounding value used for heatup and cooldown.

*** This number is increased to include the zero pressure time points of leak test and hydrotest events.

**** Increased from 0 to 1 cycle to bound possible future cycles.

5.2.4 Heat Transfer Coefficients

Heat transfer coefficients were not provided in the sources of information that were used to derive transient definitions. Conservative values were calculated by SI based on the temperatures and flow rate histories. For the hot leg and charging piping and nozzle, the following equation was used for turbulent flow in tubes, which is also bounding for stratification conditions.

$$Nu = 0.023 Re^{0.8} Pr^{0.4}, \text{ where}$$

Nu = Nusselt number = hD/k
 Re = Reynolds number = VD/ν
 Pr = Prandtl number, non-dimensional
 h = heat transfer coefficient
 D = inside diameter
 k = thermal conductivity
 V = velocity, ft/sec = $Q/(\pi D^2/4)$
 Q = volumetric flow rate
 ν = kinematic viscosity

For conditions where there is little to no surge line flow, there is swirl penetration from the RCS hot leg such that forced convection equations are appropriate. Guidance was taken from the EPRI MRP document MRP-132 [13] and MRP-146S [14]. The Reynolds number is calculated based on swirl velocity, $\Omega(x)$, which is given by:

$$\Omega(x) = (2U/D)[\Omega_0 D/(2U)]/[1 + (x/D)/(L_\Omega/D)]^\beta, \text{ where}$$

$$\Omega_0 D/(2U) = 0.63(D/D_R)$$

$$L_\Omega/D = 3.2$$

$$\beta = 1.4$$

U = RCS flow velocity

D = branch inside diameter

D_R = RCS diameter

x = axial distance from the RCS inside surface

The equation simplifies to:

$$\Omega(x) = \Omega_0/[1 + (x/D)/(3.2)]^{1.4}, \text{ where}$$

$$\Omega_0 = 1.26U/D_R$$

The formulae for Reynolds number based on the swirl flow and heat transfer coefficient are as follows:

$$Re = \frac{1}{2} \frac{\Omega D^2}{\nu}$$

$$h = 0.023 Re^{0.8} Pr^{0.3} (k/D) \quad (\text{for } Re > 10,000)$$



Table 5-8 summarizes all heat transfer coefficients that will be applied for the thermal transient analysis of the nozzle.

Table 5-8. Summary of RCS Hot Leg Surge Nozzle Heat Transfer Coefficients, Btu/hr-ft²-°F

Transients	Surge	Thermal	Hot leg
Inadvertent RCS depress./RCS group	15,169	16,864	6,411
All others	1,447	1,962	6,411

5.2.5 Piping Interface Loads

5.2.5.1 Branch Piping

Stratification and thermal expansion moments were taken from the NSP/WPS surge stratification fatigue analysis [21, p. 14 of 26]. The moments reflect the surge line bottoming out at whip restraints, which were subsequently repositioned. Using these past values for the life of the plant is conservative and bounding.

OBE moments are taken from the same analysis [21, p. 7 of 26]. The values listed for OBE are conservative for all points in the surge line. Table 5-9 lists the piping interface loads described above.

Table 5-9. RCS Hot Leg Surge Nozzle Piping Interface Loads, in-kips

Loading	Mx	My	Mz
0°F stratification	-78	-389	9
36°F stratification	-37	-1447	90
203°F stratification	884	-1033	-186
320°F stratification	1673	-618	-529
Surge pipe at 653°F	-95	-1625	1
OBE	600	200	200

OBE was specified to have 1 occurrence (60 year projected) with 50 cycles each. OBE was conservatively assumed to occur simultaneously with any transient, up to the total number of OBE events.



5.2.5.2 Run Piping

Conservative run piping interface loads for thermal expansion and OBE loading conditions were developed [26]. These loads at the branch nozzle location were not specifically tabulated in the available design input. However, interface loads were available at other sections of the same runs of piping. Standard structural analysis methodologies were utilized to calculate bounding interface load values at the location of interest. SRSS values were computed and assumed to be applied in the worst case orientation, as shown on Figure 4-3, to maximize the fatigue usage for conservatism.

The KPS replacement steam generator project contained the latest piping analysis of record for the RCL. Piping interface loads for thermal expansion and seismic loading conditions were contained in this report and were calculated based on a piping model of the RCL. Seismic OBE values are one half the seismic SSE values.

The thermal expansion values for the hot leg were assumed to represent conditions going from a stress-free temperature of 70°F to a design basis temperature of 606.8°F. The SRSS thermal moment for the RCS hot leg surge nozzle was calculated to be 2320.456 in-kip. Based on the temperature of the hot leg, THOT, the thermal run piping moment at the hot leg surge nozzle, Mhlsrg_thm, may be calculated as:

$$\text{Mhlsrg_thm} = (\text{THOT} - 70) / (606.8 - 70) \cdot 2320.456 \text{ in-kip}$$

The OBE run piping moment at the hot leg surge nozzle was calculated to be 522.390 in-kip, and can reverse direction in equal magnitude.

5.3 Thermal and Mechanical Analyses

5.3.1 Methodology Overview

ANSYS [8] FEA was used to compute transient and static stresses for input to the fatigue calculations [25]. In computing transient (time-dependent) stresses a thermal analysis was first performed to compute temperature distributions throughout the model over time. The temperatures were then used to compute thermal stresses using standard, linear elastic FEA



methodology. The following is a summary of the overall process used to perform the thermal and mechanical analyses.

- Apply bulk temperatures and heat transfer coefficients on defined convection surfaces to compute temperature distributions over time for all thermal transients.
- Perform stress analyses using temperature distribution results with the thermal sleeve (non-structural attachment) and water annulus (non-structural) removed.
- Perform stress analysis of unit internal pressure load case with thermal sleeve attachment and water annulus removed.
- Perform stress analyses of piping interface loads with thermal sleeve attachment and water annulus removed.
- Review stress results and select analysis sections (“paths”) along discontinuities and with high stress intensities.
- Extract linearized stresses at selected paths.

5.3.2 Boundary Conditions

5.3.2.1 Thermal Boundary Conditions

Due to symmetry, thermal transients were analyzed using a quarter model, as shown on Figure 5-1. Convection surfaces were defined in the loads calculation package [22] for the piping, thermal sleeve and RCS header regions. ANSYS macro files were created to apply temperature and film coefficients to the various convections surfaces, which are shown on Figure 5-4.

5.3.2.2 Mechanical Boundary Conditions

Symmetry and displacement boundary conditions were applied to the cut surfaces of the quarter model, as shown on Figure 5-5.



The edges of the surge piping and the hot leg piping were coupled in the axial (longitudinal) direction to prevent gross distortion of the cross sections and simulate the connected piping. The coupled conditions are shown on Figure 5-5.

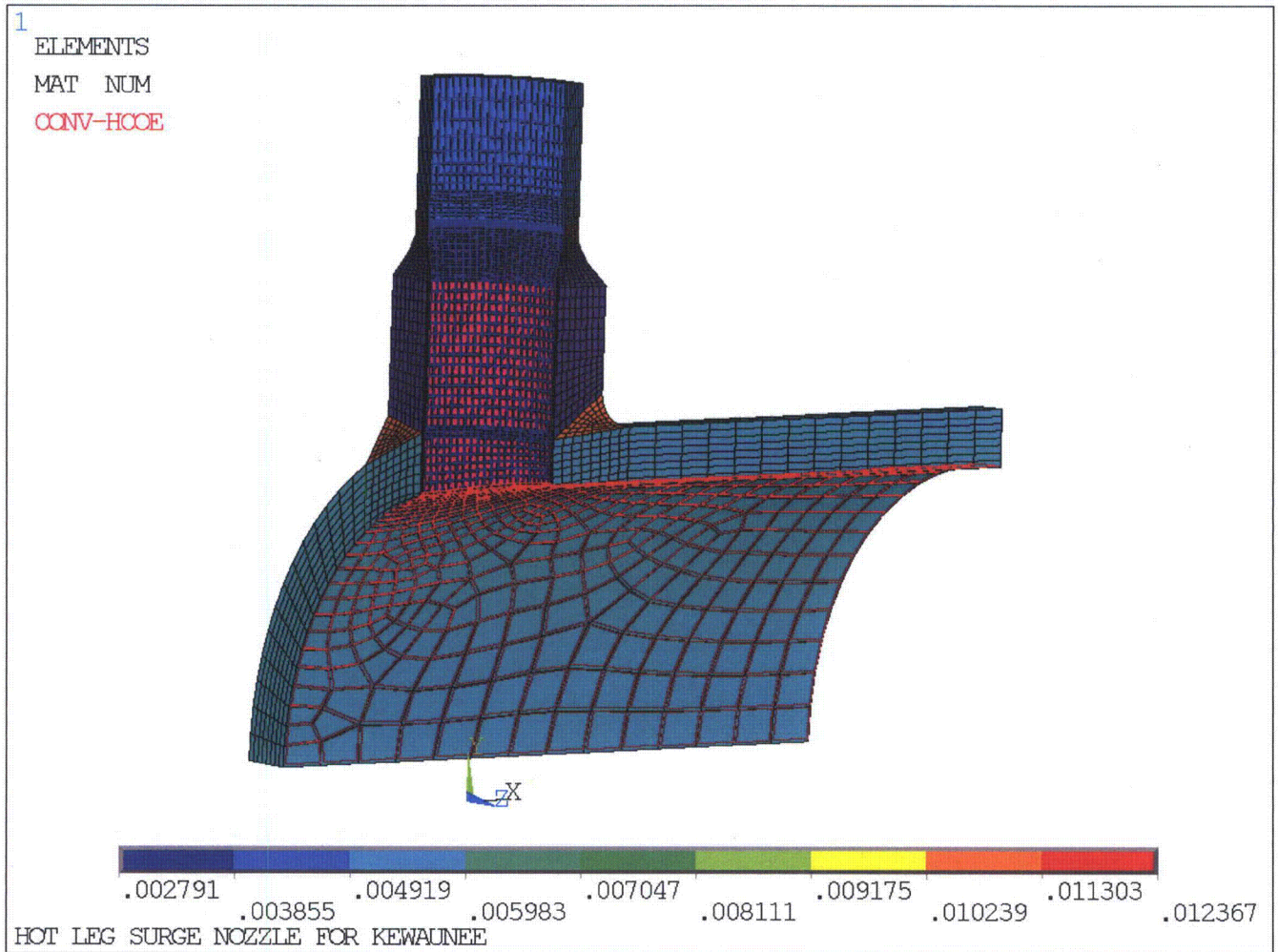


Figure 5-4. RCS Hot Leg Surge Nozzle Convection Surfaces

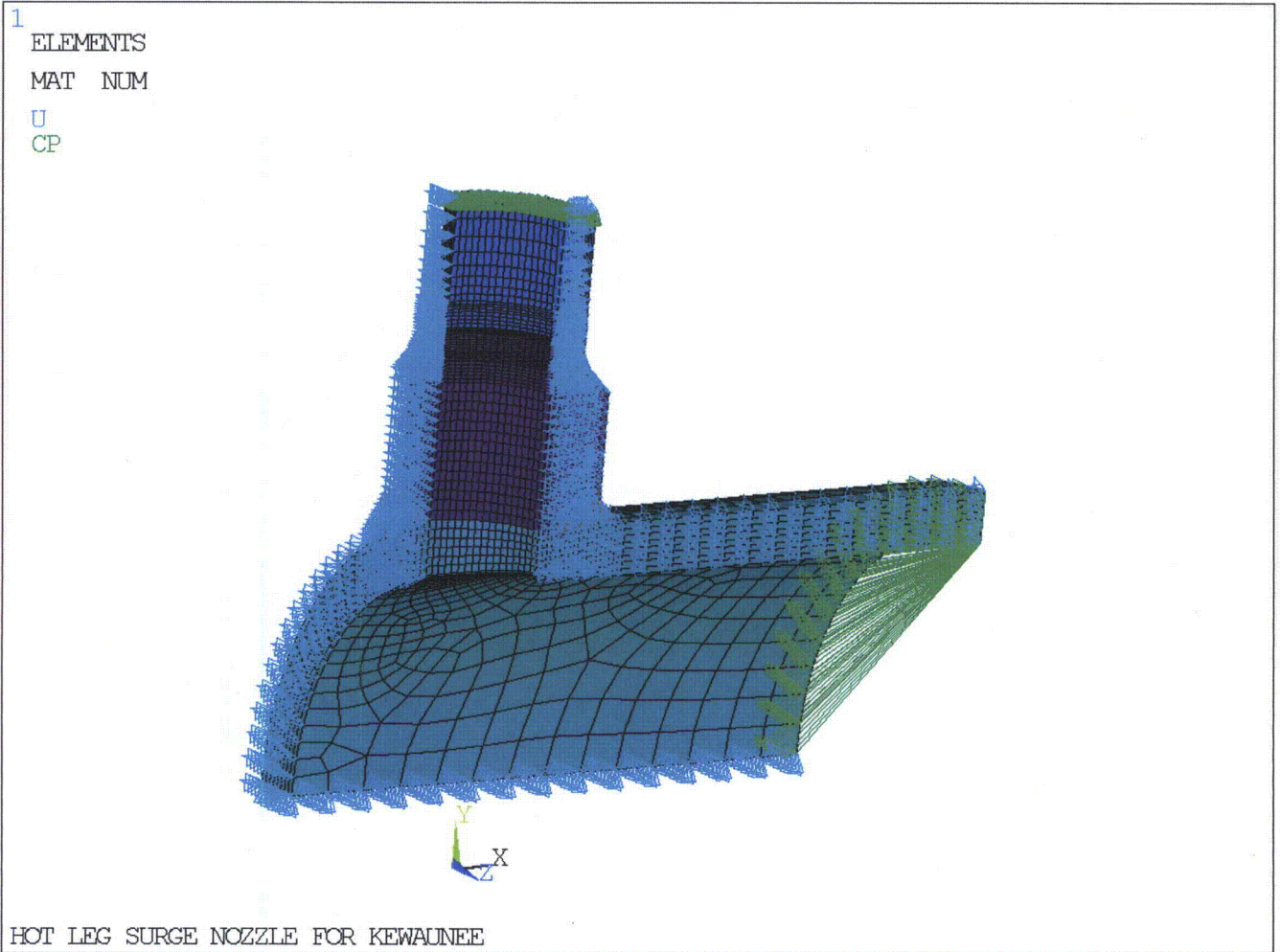


Figure 5-5. RCS Hot Leg Surge Nozzle Mechanical Boundary Conditions

5.3.3 Internal Pressure Analysis

A unit (1 psig) internal pressure analysis was performed so that results could be scaled to any internal pressure condition, based on linear elastic analysis. The pressure surfaces are shown on Figure 5-6. Cap loads were applied on the surge piping and the hot leg piping, based on multiplying the unit pressure by the ratio of the fluid cross sectional area to the metal cross sectional area. Values are negative to simulate tensile stress.

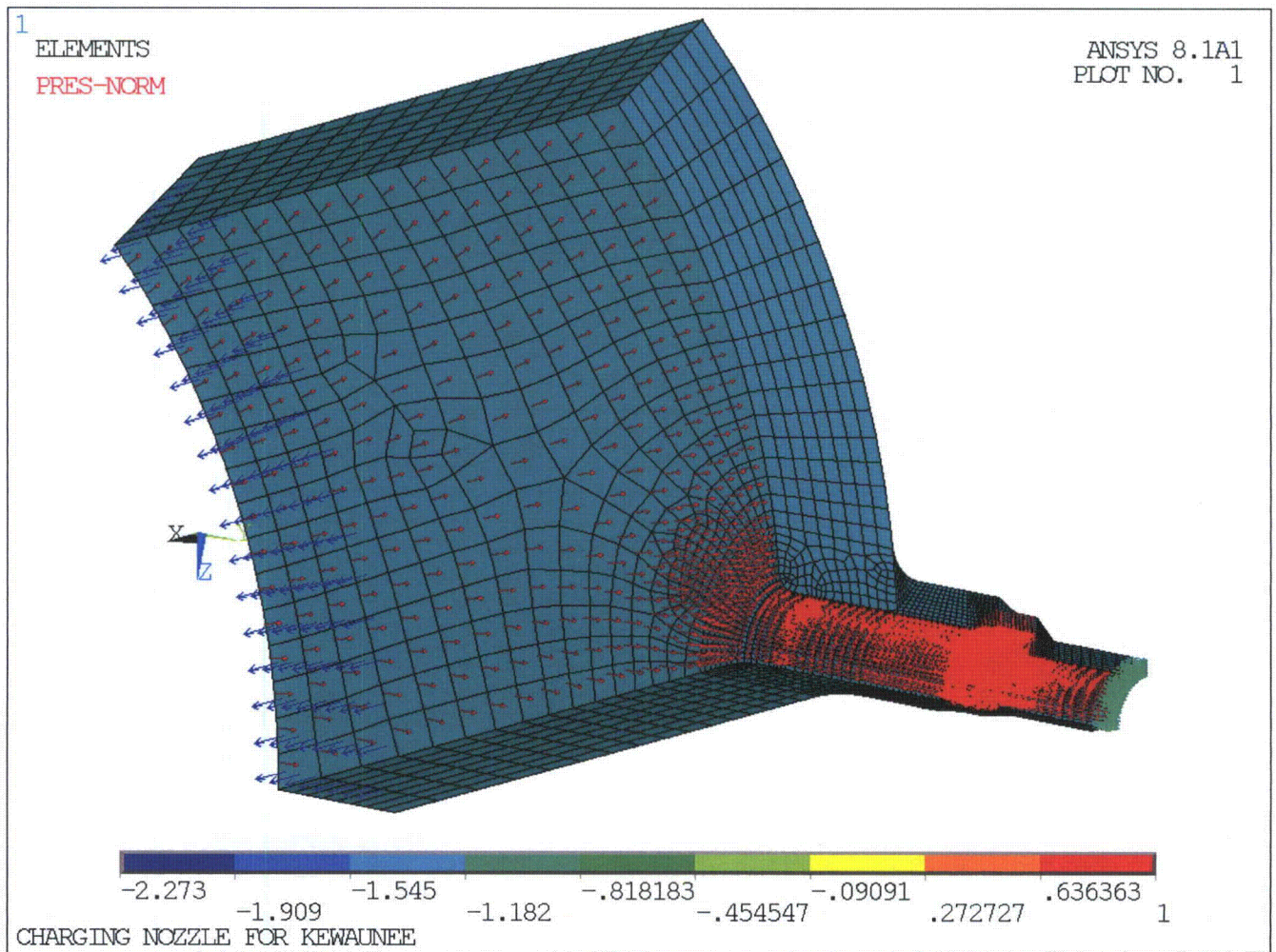


Figure 5-6. RCS Hot Leg Surge Nozzle Unit Internal Pressure Application

5.3.4 Piping Interface Loading Analysis

5.3.4.1 Branch Piping

Table 5-9 lists branch piping interface loads for thermal and OBE conditions. For the stress analysis the loads were transformed into a coordinate system consistent with that of the FEA.

In order to apply these asymmetric loads, a full model was created from the quarter model using symmetry commands in ANSYS. The model is shown on Figure 5-7. A pilot node was created at the neutral axis of the surge piping along with a defined contact surface to apply the loads on the model.

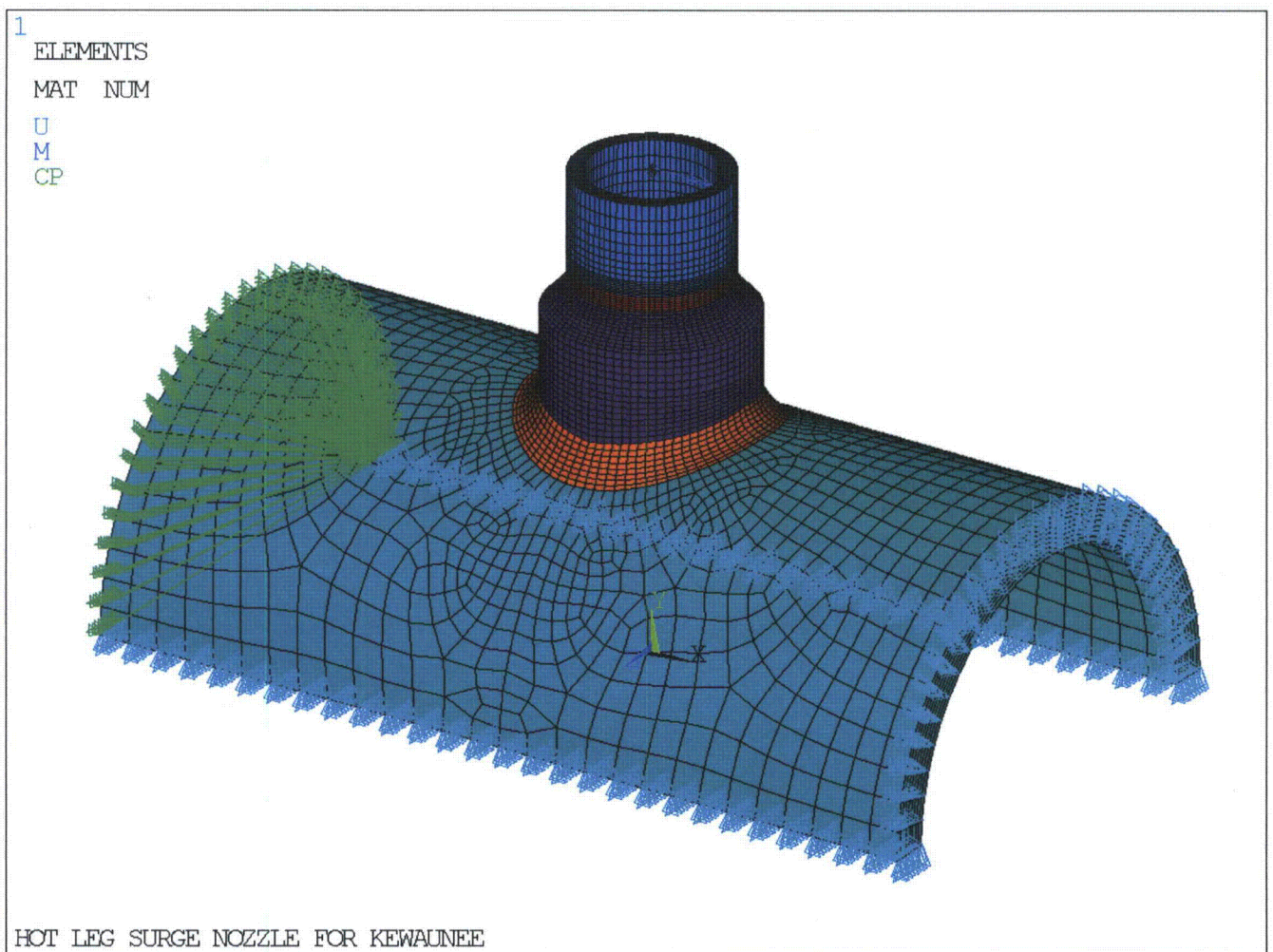


Figure 5-7. RCS Hot Leg Surge Nozzle Full Finite Element Model

The boundary conditions were similar to the quarter model, except that the edge of the surge piping was not coupled in the circumferential direction in order to allow rotation of the pipe due to bending. The cut surfaces of hot leg piping had symmetry boundary conditions applied, the longitudinal direction of one edge of the hot leg piping had rollers applied, and the other side of the hot leg piping was coupled in the longitudinal direction to allow expansion but prevent gross distortion of the cross section to simulate the connected piping.

A benchmark analysis to verify proper application of the pilot node methodology was also conducted in [25] using a unit moment. The FEA computed axial stress was compared to that computed using a standard structural mechanics equation. The ANSYS result matched the hand calculation to within 1% and was considered to be more accurate, as it reflected the effects of gross structural discontinuities in the overall structure. Therefore the FEA methodology was confirmed to be appropriately executed.

5.3.4.2 Run Piping

Run piping loads were evaluated using the same methodology described in Section 4.3.4.2.

5.3.5 Thermal Transients

The thermal stress analyses were performed by ANSYS using the temperature distributions computed in the thermal analyses for various time steps of each defined transient.

5.3.6 Selection of Analysis Sections (Paths)

Seven stress linearization paths, PATH1 through PATH7, were chosen for fatigue analysis. Stress paths are defined around regions of discontinuities and at areas of high stress. The paths are shown on Figure 5-8 through Figure 5-11.



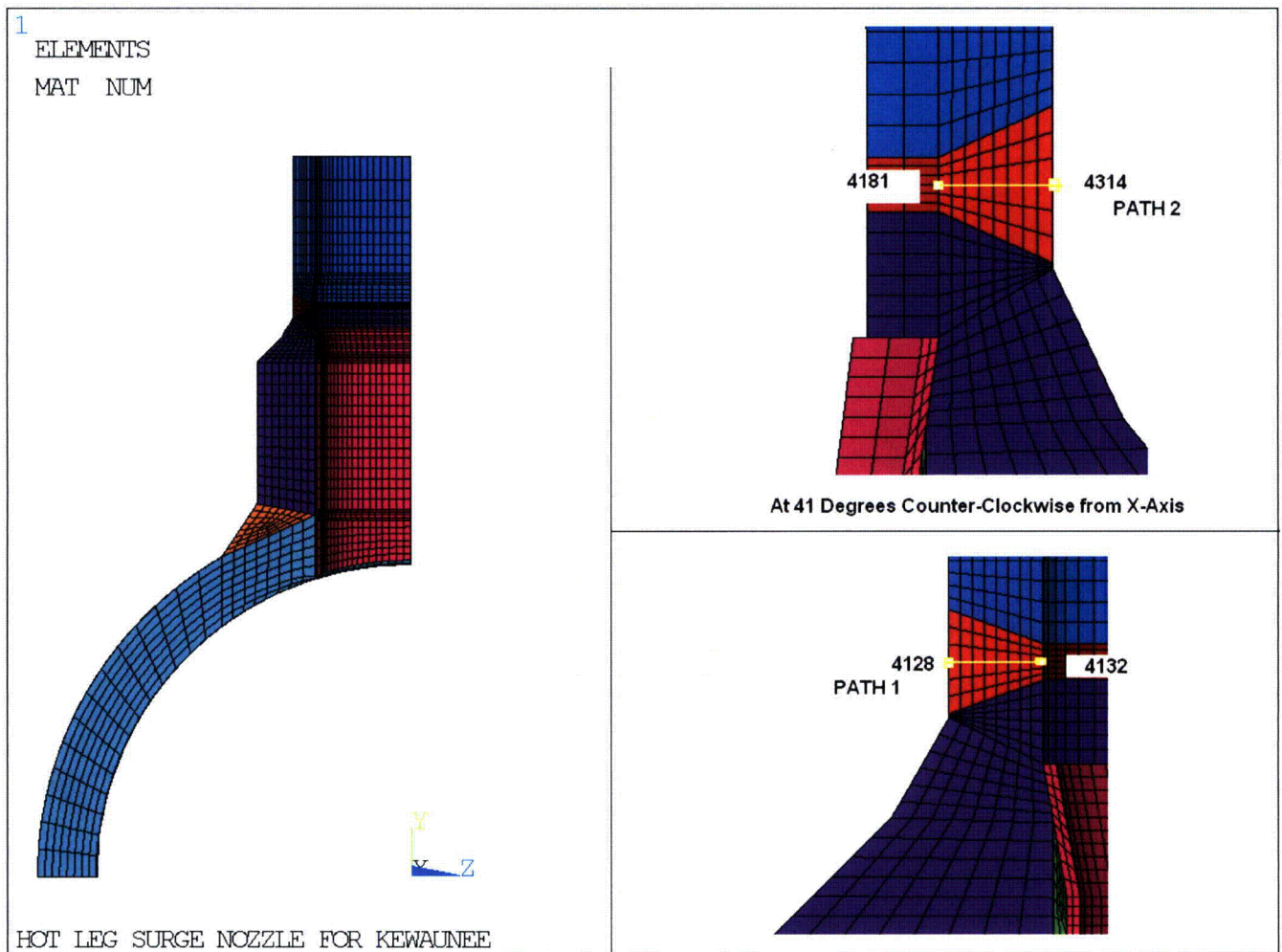


Figure 5-8. RCS Hot Leg Surge Nozzle Stress Linearization PATH1 and PATH2

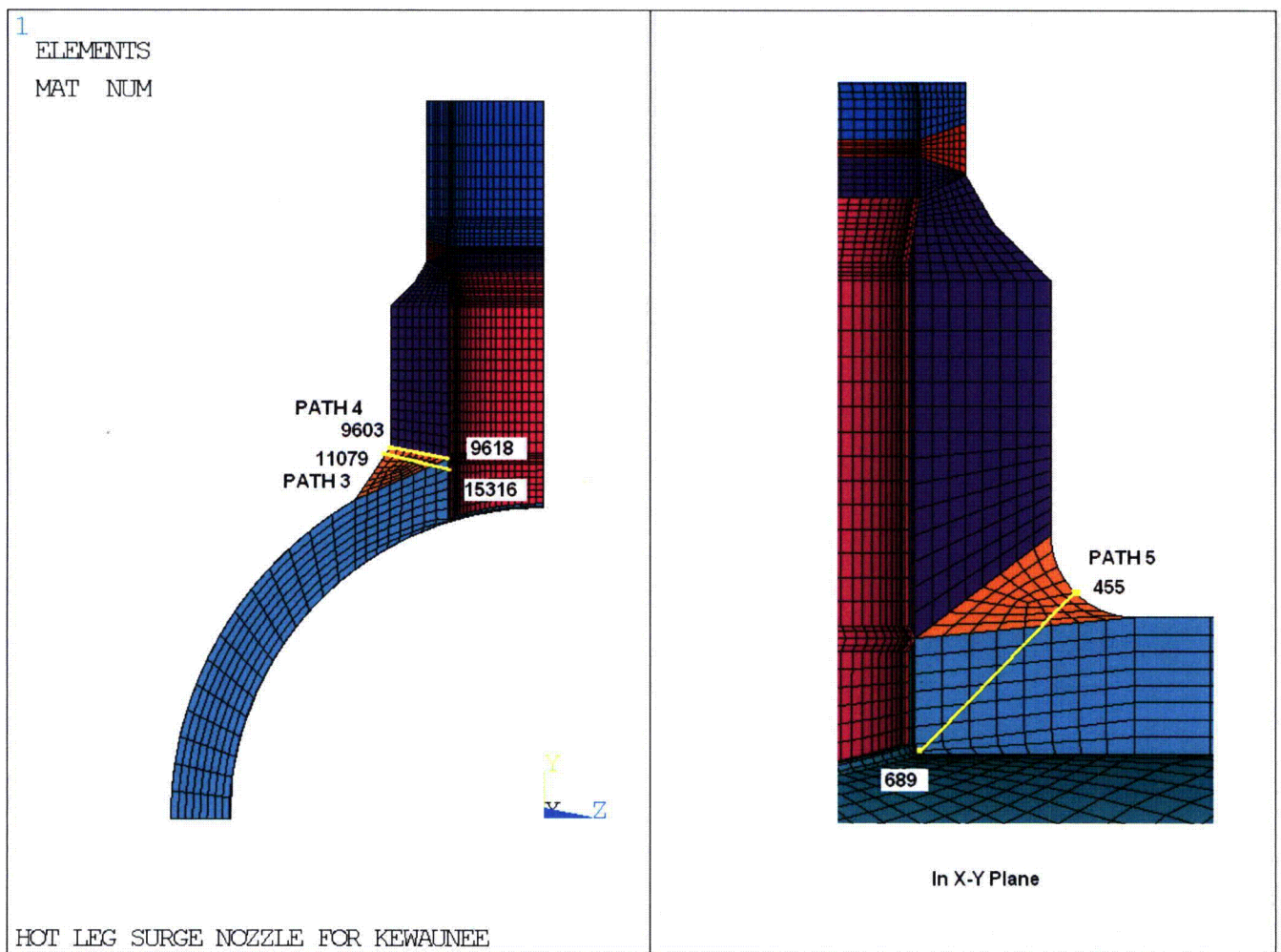


Figure 5-9. RCS Hot Leg Surge Nozzle Stress Linearization PATH3 through PATH5

Note: The two faces shown are 90 degrees out-of-phase.
The inside node is located on the inside face of the nozzle/piping for all paths.

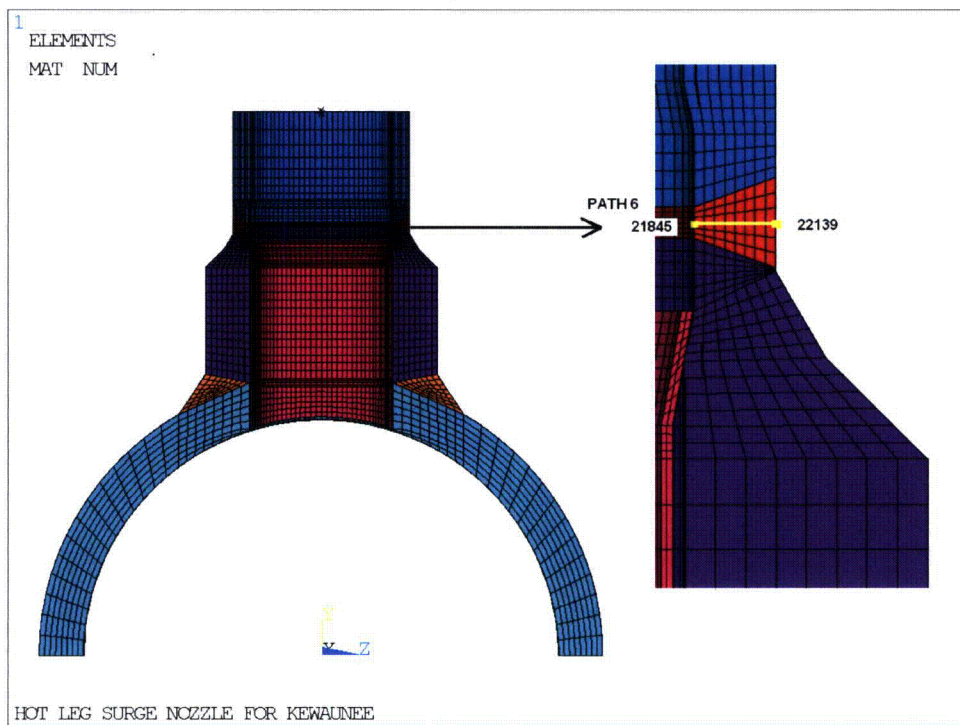


Figure 5-10. RCS Hot Leg Surge Nozzle Stress Linearization PATH6

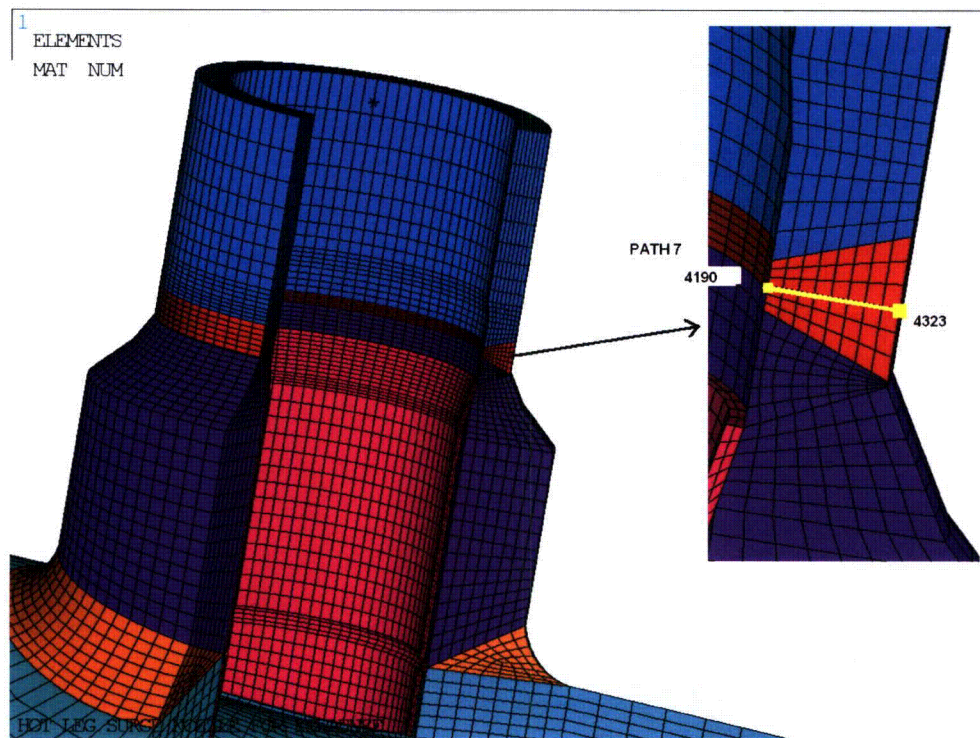


Figure 5-11. RCS Hot Leg Surge Nozzle Stress Linearization PATH7

5.3.7 Summary of FEA Analyses

Table 5-10 summarizes the various ANSYS thermal and mechanical analyses and post-processing operations performed to support the fatigue evaluation of the KPS hot leg surge nozzle.

Table 5-10. Summary of RCS Hot Leg Surge Nozzle ANSYS Load Cases

Hot Leg Surge Nozzle Bounding Transients -- Symmetric Loading on Quarter Model						
ANSYS						
#	Label	Description	Input Files		Output Files	
			Thermal	Stress	Post	Notes
Hot Leg Surge Nozzle Transients, As Analyzed						
1	TRAN1	RCS Heatup	TRAN1-T.INP	TRAN1-S.INP	LIN-STR.INP	TRAN1-S-S# LIN
2	TRAN2	RCS Cutdown	TRAN2-T.INP	TRAN2-S.INP	LIN-STR.INP	TRAN2-S-S# LIN
3	TRAN3	Plant Loading at 5% Power/Minute	TRAN3-T.INP	TRAN3-S.INP	LIN-STR.INP	TRAN3-S-S# LIN
4	TRAN4	Plant Unloading at 5% Power/Minute	TRAN4-T.INP	TRAN4-S.INP	LIN-STR.INP	TRAN4-S-S# LIN
5	TRAN5	RCS Group	TRAN5-T.INP	TRAN5-S.INP	LIN-STR.INP	TRAN5-S-S# LIN
6	TRAN6	Inadvertent RCS Depress/Aux Spray	TRAN6-T.INP	TRAN6-S.INP	LIN-STR.INP	TRAN6-S-S# LIN
7	TRAN7	PZR Outsurge Transients (PIO 150)	TRAN7-T.INP	TRAN7-S.INP	LIN-STR.INP	TRAN7-S-S# LIN
8	TRAN8	PZR Outsurge Transients (PIO 150H)	TRAN8-T.INP	TRAN8-S.INP	LIN-STR.INP	TRAN8-S-S# LIN
9	TRAN9	Refueling	--	--	--	--
10	TRAN10	Primary Side Leak test	--	--	--	--
11	TRAN11	Primary Side Hydrostatic test	--	--	--	--
Scale results based on the unit pressure case						
Hot Leg Surge Nozzle Static Load Cases						
#	Label	Description	Stress	Post	Output	Notes
1	UNTPRESS	1 psig internal pressure	PRESS.INP	LIN-STR.INP	PRESS-S# LIN	Analyzed at stress free, uniform temperature of 70°F on FE quarter model.
2	MOMENT (Mx)	Branch piping interface loads	MOM_X.INP	LIN-STR.INP	MOM_X-S# LIN	Analyzed at stress free uniform temperature of 70°F on FE 180 Deg model.
3	MOMENT (Mz)	Branch piping interface loads	MOM_Z.INP	LIN-STR.INP	MOM_Z-S# LIN	
4	TORSION (My)	Branch piping interface loads	TORSION.INP	LIN-STR.INP	TORSION-S# LIN	
# = 1 for PATH1, 2 for PATH2, 3 for PATH3, 4 for PATH4, 5 for PATH5, 6 for PATH6, 7 for PATH7, 8 for PATH8						



5.4 ASME Code Fatigue Calculations

5.4.1 Fatigue Calculations

5.4.1.1 Stress Calculations

Fatigue calculations that credit water solid operation into the future and utilize 60-year projected cycles were performed in the Reference [24] calculation package using the methodology summarized in Section 3.1 of this report. In the first phase fatigue analysis [23] that conservatively assumed modified steam bubble method of operation for the entire history and design cycle counts, the bounding fatigue was determined to be located at PATH1, 2, 6, and 7, which are all located at the nozzle to surge piping field butt weld. Note that this is the same critical region as that identified for the "Older Vintage Westinghouse Plant" in NUREG/CR-6260 [2, Section 5.4.3].

For these selected paths, FSRFs were applied to the membrane plus bending (M+B) stress components. These FSRFs were conservatively applied to all six components (three normal, three shear) of the stress tensor. The following factors were chosen by taking guidance from the local stress indices (K indices) from NB-3600, as follows [1, Table NB-3681(a)-1]:

Pressure: 1.2
Moment: 1.8
Thermal: 1.7

In addition, the peak thermal stress components (PEAK) were added back into the total stress to capture the peak stress due to nonlinear radial temperature gradient, as required by Table NB-3217-2 of the ASME Code [1], as follows:

$$P+Q+F = (\text{ANSYS M+B})\text{FSRF} + (\text{ANSYS PEAK})$$

The loads package [22] provides temperature parameters and pressure for the specified thermal transients. Unit pressure stresses were scaled by the ratio of gage pressure to the analyzed unit pressure of 1000 psi. For branch piping moments, unit stresses are scaled based on moment magnitudes, surge piping temperature, and stratification magnitude. Moments were converted from the Westinghouse coordinate system to the ANSYS coordinate system.

5.4.1.2 Load Sets

Transients that consist of both stress peaks and valleys are split so that each successive peak or valley is treated as a separate load set. Table 5-11 shows the transients as input to VESLFAT. Each pressurizer insurge outsurge (I/O) event consists of three outsurge load sets and one insurge (steady state) load set.

Table 5-11. Hot Leg Surge Nozzle Load Sets as Input to VESLFAT

Load Sets*	Event	Abbreviation	60-Year Projected Cycles
1	RCS Heatup	Heatup	110
2	RCS Cooldown	Cooldown	110
3 – 5	Plant Loading at 5% Power/Minute	PlntLoad	214
6, 7	Plant Unloading at 5% Power/Minute	PlntUnload	150
8 – 10	RCS Group	RCSGRP	244
11, 12	Inadvertent RCS Depress./Aux Spray	InadvRCSDep	1
13 – 16	PIO334	PIO334	1
17 – 20	PIO331	PIO331	1
21 – 24	PIO321	PIO321	2
25 – 28	PIO304	PIO304	18
29 – 32	PIO285	PIO285	31
33 – 36	PIO275	PIO275	32
37 – 40	PIO250	PIO250	8
41 – 44	PIO200	PIO200	66
45 – 48	PIO175	PIO175	80
49 – 52	PIO150	PIO150	639
53 – 56	PIO150H	PIO150H	348
57 – 60	PIO210	PIO210	107
61 – 64	PIO177	PIO177	102
65	Refueling	Refueling	87
66	Primary Side Leak Test	LeakTest	48
67	Primary Side Hydrostatic Test	HydroTest	2
68	Operating Basis Earthquake	OBE	1

* For events with multiple temperature or pressure peaks and valleys, events are split into multiple load sets based on a review of the combined stress magnitudes, so that each significant stress peak or valley is a separate load set.

5.4.1.3 Material Properties

Table 5-12 lists the temperature-dependent material properties used in the analysis, and Table 5-13 lists the fatigue curve for stainless steel materials [1, Appendix I, Tables I-9.1 (Figure I-9.2.1) and I-9.2.2 (Curve C)]. At welds, the material that has lower S_m values is used. VESLFAT automatically scales the stresses by the ratio of E on the fatigue curve to E in the analysis, for purposes of determining allowable numbers of cycles, as required by the ASME Code.

Table 5-12. RCS Hot Leg Surge Nozzle Material Properties for Fatigue Analysis

Material	T, °F	E _{analysis} , ksi	S _m , ksi
TP316SS	70	28,300	20.0
	200	27,600	20.0
	300	27,000	20.0
	400	26,500	19.2
	500	25,800	17.9
	600	25,300	17.0
	650	25,050	16.6
	700	24,800	16.3

Table 5-13. RCS Hot Leg Surge Nozzle Stainless Steel Fatigue Curve for Fatigue Analysis

Number of Cycles	S _a , ksi
10	708
20	512
50	345
100	261
200	201
500	148
1,000	119
2,000	97
5,000	76
10,000	64
20,000	55.5
50,000	46.3
100,000	40.8
200,000	35.9
500,000	31
1,000,000	28.2
2,000,000	22.8
5,000,000	18.4
10,000,000	16.4
20,000,000	15.2
50,000,000	14.3
100,000,000	14.1
1,000,000,000	13.9
10,000,000,000	13.7
100,000,000,000	13.6

5.4.1.4 Results

Initial fatigue calculations were made for all four selected paths, to determine the one with the highest CUF.

Table 5-14 summarizes the initial fatigue usage results at the inside surface.



Table 5-14. Charging Nozzle Fatigue Usage Results (no OBE)

Path	CUF
1	0.040
2	0.110
6	0.126
7	0.123

Since paths 6 and 7 are bounding, they were selected for more detailed analysis. For the second fatigue usage analysis at the bounding locations, OBE is combined with one of the load sets [13, PIO334OUT] in the load set pair that has the highest S_{alt} value. Table 5-15 and Table 5-16 present the detailed results for the second runs, showing each load set pair for each run that contributes to the total fatigue usage.

Table 5-15. RCS Hot Leg Surge Nozzle Detailed CUF Results for PATH6 (+OBE)

I	Load Set A	Load Set B	S _m , psi	K _e	S _{alt} , psi	n	N	Usage
1	13 PIO334OUT	14 PIO334OUT	65236	1.558	100410	1	1779	0.000562
2	17 PIO331OUT	18 PIO331OUT	63946	1.481	93391	1	2306	0.000434
3	21 PIO321OUT	22 PIO321OUT	63601	1.460	91592	2	2481	0.000806
4	25 PIO304OUT	26 PIO304OUT	63021	1.426	88594	18	2811	0.006403
5	29 PIO285OUT	30 PIO285OUT	62382	1.388	85340	31	3235	0.009582
6	33 PIO275OUT	34 PIO275OUT	62050	1.368	83666	32	3485	0.009182
7	37 PIO250OUT	38 PIO250OUT	61233	1.319	79604	8	4201	0.001904
8	41 PIO200OUT	42 PIO200OUT	59667	1.226	72033	66	6207	0.010634
9	45 PIO175OUT	46 PIO175OUT	58922	1.181	68536	80	7587	0.010545
10	49 PIO150OUT	50 PIO150OUT	58210	1.139	65250	639	9250	0.069085
11	57 PIO210OUT	58 PIO210OUT	49075	1	48984	107	37604	0.002845
12	61 PIO177OUT	62 PIO177OUT	44013	1	44194	102	64538	0.001581
13	8 RCSGRP	9 RCSGRP	35727	1	38095	244	145017	0.001683
14	3 PlntLoad	12 InadvRCSDep	31510	1	33369	1	315711	0.000003
15	3 PlntLoad	54 PIO150HOUT	30395	1	32665	213	360657	0.000591
16	53 PIO150HOUT	54 PIO150HOUT	30227	1	32461	135	375044	0.000360
17	15 PIO334OUT	53 PIO150HOUT	29497	1	30817	1	522115	0.000002
18	19 PIO331OUT	53 PIO150HOUT	29372	1	30691	1	538118	0.000002
19	23 PIO321OUT	53 PIO150HOUT	28959	1	30269	2	595403	0.000003
20	27 PIO304OUT	53 PIO150HOUT	28258	1	29555	18	709225	0.000025
21	31 PIO285OUT	53 PIO150HOUT	27477	1	28758	31	866326	0.000036
22	35 PIO275OUT	53 PIO150HOUT	27067	1	28340	32	964513	0.000033
23	39 PIO250OUT	53 PIO150HOUT	26043	1	27295	8	1112200	0.000007
24	43 PIO200OUT	53 PIO150HOUT	24010	1	25219	66	1439600	0.000046
25	7 PlntUnload	53 PIO150HOUT	23554	1	25012	54	1478800	0.000037
26	7 PlntUnload	65 Refueling	22054	1	17865	87	5973400	0.000015
27	1 Heatup	7 PlntUnload	20540	1	17131	9	7690100	0.000001
28	1 Heatup	4 PlntLoad	19731	1	16663	101	9086800	0.000011
29	6 PlntUnload	59 PIO210OUT	15721	1	16421	107	9923600	0.000011
30	6 PlntUnload	47 PIO175OUT	15206	1	16085	43	11937000	0.000004
31	2 Cooldown	4 PlntLoad	18571	1	15442	110	17314000	0.000006
32	4 PlntLoad	47 PIO175OUT	14820	1	14834	3	28845000	0.000000
33	68 OBE	68 OBE	15939	1	14345	1	47691000	0
34	11 InadvRCSDep	47 PIO175OUT	14193	1	14054	1	169530000	0
35	5 PlntLoad	47 PIO175OUT	13693	1	13759	33	505230000	0
							Total =	0.126436

Table 5-16. RCS Hot Leg Surge Nozzle Detailed CUF Results for PATH7 (+OBE)

I	Load Set A	Load Set B	S_m , psi	K_e	S_{alt} , psi	n	N	Usage
1	13 PIO334OUT	14 PIO334OUT	68831	1.772	120357	1	965	0.001037
2	17 PIO331OUT	18 PIO331OUT	64236	1.498	94909	1	2171	0.000461
3	21 PIO321OUT	22 PIO321OUT	63863	1.476	92952	2	2347	0.000852
4	25 PIO304OUT	26 PIO304OUT	63238	1.439	89706	18	2683	0.006710
5	29 PIO285OUT	30 PIO285OUT	62545	1.397	86166	31	3120	0.009935
6	33 PIO275OUT	34 PIO275OUT	62186	1.376	84348	32	3381	0.009466
7	37 PIO250OUT	38 PIO250OUT	61299	1.323	79932	8	4137	0.001934
8	41 PIO200OUT	42 PIO200OUT	59592	1.221	71689	66	6328	0.010430
9	45 PIO175OUT	46 PIO175OUT	58777	1.173	67871	80	7891	0.010138
10	49 PIO150OUT	50 PIO150OUT	57994	1.126	64276	639	9828	0.065017
11	57 PIO210OUT	58 PIO210OUT	49240	1	49146	107	36982	0.002893
12	61 PIO177OUT	62 PIO177OUT	44152	1	44330	102	63459	0.001607
13	8 RCSGRP	9 RCSGRP	34890	1	37242	244	163939	0.001488
14	3 PlntLoad	54 PIO150HOUT	30574	1	32847	214	348360	0.000614
15	53 PIO150HOUT	54 PIO150HOUT	30433	1	32669	134	360375	0.000372
16	12 InadvRCSDep	53 PIO150HOUT	30354	1	32150	1	398326	0.000003
17	15 PIO334OUT	53 PIO150HOUT	29192	1	30513	1	561411	0.000002
18	19 PIO331OUT	53 PIO150HOUT	29061	1	30380	1	579769	0.000002
19	23 PIO321OUT	53 PIO150HOUT	28622	1	29933	2	646111	0.000003
20	27 PIO304OUT	53 PIO150HOUT	27879	1	29176	18	779576	0.000023
21	31 PIO285OUT	53 PIO150HOUT	27048	1	28331	31	966759	0.000032
22	35 PIO275OUT	53 PIO150HOUT	26613	1	27886	32	1037200	0.000031
23	39 PIO250OUT	53 PIO150HOUT	25524	1	26777	8	1184000	0.000007
24	7 PlntUnload	53 PIO150HOUT	23167	1	24619	120	1557200	0.000077
25	7 PlntUnload	65 Refueling	22533	1	18405	30	4994200	0.000006
26	4 PlntLoad	65 Refueling	21682	1	17817	57	6070000	0.000009
27	1 Heatup	4 PlntLoad	19860	1	16791	110	8677400	0.000013
28	6 PlntUnload	43 PIO200OUT	15731	1	16588	66	9337800	0.000007
29	4 PlntLoad	59 PIO210OUT	16228	1	16319	47	10461000	0.000005
30	6 PlntUnload	55 PIO150HOUT	15270	1	16115	84	11735000	0.000007
31	5 PlntLoad	59 PIO210OUT	15363	1	15467	60	17063000	0.000004
32	2 Cooldown	55 PIO150HOUT	17456	1	14267	110	55943000	0.000002
33	11 InadvRCSDep	55 PIO150HOUT	14124	1	13960	1	501190000	0
34	5 PlntLoad	47 PIO175OUT	13564	1	13634	80	45204000000	0
35	68 OBE	68 OBE	14898	1	13408	1	infinite	0
Total =								0.123186

To reduce excess conservatism, S_m averaging was applied to those load set pairs with $K_e > 1.0$ and for which secondary stress is due only to temperature transients or restraint of free end deflection, in accordance with Note 3 of ASME Code Figure NB-3222-1. Since Pair 1 includes OBE, and Pairs 11 and higher have $K_e = 1.0$, S_m averaging was applied to Pairs 2 through 10. The following apply to all of these pairs:

S_m used in VESLFAT = 18628 psi
Maximum temperature = 455°F
 S_m at 455°F = 18485 psi
Minimum temperature = 140°F

S_m at 140°F = 20000 psi
Average S_m = 19242.5 psi

Table 5-17 and Table 5-18 show the revised K_e , S_{alt} , and usage calculations. Note that K_e before S_m averaging was recalculated as a check.

Table 5-17. RCS Hot Leg Surge Nozzle Detailed Fatigue Results for PATH6 (+OBE & S_m averaging)

I	Load Set A	Load Set B	S_m , psi	Previous K_e	Refined K_e	S_{alt} , ksi	n	N	Usage
1	13 PIO334OUT	14 PIO334OUT							0.000562
2	17 PIO331OUT	18 PIO331OUT	63946	1.4809	1.3591	85.709	1	3183	0.000314
3	21 PIO321OUT	22 PIO321OUT	63601	1.4603	1.3392	83.993	2	3434	0.000582
4	25 PIO304OUT	26 PIO304OUT	63021	1.4257	1.3057	81.134	18	3911	0.004602
5	29 PIO285OUT	30 PIO285OUT	62382	1.3876	1.2688	78.032	31	4528	0.006846
6	33 PIO275OUT	34 PIO275OUT	62050	1.3678	1.2496	76.436	32	4894	0.006539
7	37 PIO250OUT	38 PIO250OUT	61233	1.3191	1.2024	72.565	8	6025	0.001328
8	41 PIO200OUT	42 PIO200OUT	59667	1.2256	1.1120	65.353	66	9191	0.007181
9	45 PIO175OUT	46 PIO175OUT	58922	1.1812	1.0690	62.024	80	11648	0.006868
10	49 PIO150OUT	50 PIO150OUT	58210	1.1387	1.0279	58.897	639	14981	0.042653
11	57 PIO210OUT	58 PIO210OUT							0.002845
12	61 PIO177OUT	62 PIO177OUT							0.001581
13	8 RCSGRP	9 RCSGRP							0.001683
14	3 PlntLoad	12 InadvRCSDep							0.000003
15	3 PlntLoad	54 PIO150HOUT							0.000591
16	53 PIO150HOUT	54 PIO150HOUT							0.000360
17	15 PIO334OUT	53 PIO150HOUT							0.000002
18	19 PIO331OUT	53 PIO150HOUT							0.000002
19	23 PIO321OUT	53 PIO150HOUT							0.000003
20	27 PIO304OUT	53 PIO150HOUT							0.000025
21	31 PIO285OUT	53 PIO150HOUT							0.000036
22	35 PIO275OUT	53 PIO150HOUT							0.000033
23	39 PIO250OUT	53 PIO150HOUT							0.000007
24	43 PIO200OUT	53 PIO150HOUT							0.000046
25	7 PlntUnload	53 PIO150HOUT							0.000037
26	7 PlntUnload	65 Refueling							0.000015
27	1 Heatup	7 PlntUnload							0.000001
28	1 Heatup	4 PlntLoad							0.000011
29	6 PlntUnload	59 PIO210OUT							0.000011
30	6 PlntUnload	47 PIO175OUT							0.000004
31	2 Cooldown	4 PlntLoad							0.000006
32	4 PlntLoad	47 PIO175OUT							0.000000
33	68 OBE	68 OBE							0
34	11 InadvRCSDep	47 PIO175OUT							0
35	5 PlntLoad	47 PIO175OUT							0
Total =									0.084777

Table 5-18. RCS Hot Leg Surge Nozzle Detailed CUF Results for PATH7 (+OBE & S_m averaging)

I	Load Set A	Load Set B	S_m , psi	Previous K_e	Refined K_e	S_{alt} , ksi	n	N	Usage
1	13 PIO334OUT	14 PIO334OUT							0.001037
2	17 PIO331OUT	18 PIO331OUT	64236	1.4982	1.3758	87.158	1	2989	0.000335
3	21 PIO321OUT	22 PIO321OUT	63863	1.4759	1.3543	85.291	2	3242	0.000617
4	25 PIO304OUT	26 PIO304OUT	63238	1.4386	1.3182	82.195	18	3725	0.004832
5	29 PIO285OUT	30 PIO285OUT	62545	1.3973	1.2782	78.819	31	4361	0.007109
6	33 PIO275OUT	34 PIO275OUT	62186	1.3759	1.2574	77.086	32	4740	0.006750
7	37 PIO250OUT	38 PIO250OUT	61299	1.3230	1.2062	72.877	8	5922	0.001351
8	41 PIO200OUT	42 PIO200OUT	59592	1.2212	1.1077	65.025	66	9379	0.007037
9	45 PIO175OUT	46 PIO175OUT	58777	1.1726	1.0606	61.391	80	12244	0.006534
10	49 PIO150OUT	50 PIO150OUT	57994	1.1259	1.0154	57.969	639	16183	0.039485
11	57 PIO210OUT	58 PIO210OUT							0.002893
12	61 PIO177OUT	62 PIO177OUT							0.001607
13	8 RCSGRP	9 RCSGRP							0.001488
14	3 PlntLoad	54 PIO150HOUT							0.000614
15	53 PIO150HOUT	54 PIO150HOUT							0.000372
16	12 InadvRCSDep	53 PIO150HOUT							0.000003
17	15 PIO334OUT	53 PIO150HOUT							0.000002
18	19 PIO331OUT	53 PIO150HOUT							0.000002
19	23 PIO321OUT	53 PIO150HOUT							0.000003
20	27 PIO304OUT	53 PIO150HOUT							0.000023
21	31 PIO285OUT	53 PIO150HOUT							0.000032
22	35 PIO275OUT	53 PIO150HOUT							0.000031
23	39 PIO250OUT	53 PIO150HOUT							0.000007
24	7 PlntUnload	53 PIO150HOUT							0.000077
25	7 PlntUnload	65 Refueling							0.000006
26	4 PlntLoad	65 Refueling							0.000009
27	1 Heatup	4 PlntLoad							0.000013
28	6 PlntUnload	43 PIO200OUT							0.000007
29	4 PlntLoad	59 PIO210OUT							0.000005
30	6 PlntUnload	55 PIO150HOUT							0.000007
31	5 PlntLoad	59 PIO210OUT							0.000004
32	2 Cooldown	55 PIO150HOUT							0.000002
33	11 InadvRCSDep	55 PIO150HOUT							0
34	5 PlntLoad	47 PIO175OUT							0
35	68 OBE	68 OBE							0
Total =									0.082292

The total CUF of 0.085 at the bounding location (PATH6) is below the ASME Code allowable limit of 1.0.

5.4.2 EAF Calculations

The EAF evaluation was performed using the Integrated Strain Rate method described in MRP-47, Rev. 1 [7, p. 4-14]. The stress intensity for the total stress from the combined stress



results was calculated for each time step, using the six stress components. Strain values in terms of percent strain were computed from the signed stress intensity values based on:

$$\varepsilon = \frac{100 * \sigma_{SI}}{E}$$

The value of Young's Modulus, E, was taken as the E of the stainless steel fatigue curve.

An environmentally-assisted fatigue factor (F_{en}) was calculated for each time step with increasing strain (becoming more tensile) in both the dominant stress direction and the total stress intensity, according to the methodology described in Section 3.2. In this process, the strain rates and strain contributions of each time step were also calculated. To determine the overall F_{en} for each transient, the summation of all tensile strain contributions for each time step was performed. Then the F_{en} for each time step was multiplied by the difference in strain amplitude between the current and previous time steps. The results of this product were summed. The F_{en} for the entire transient was calculated as follows:

$$F_{en(total)} = \frac{\sum(F_{en(individual)} \times \Delta\varepsilon)}{\sum\Delta\varepsilon}$$

Where:

$F_{en(individual)}$ = the calculated F_{en} for each time step.

$\Delta\varepsilon$ = the difference between the strain amplitude (%) of the current time step and that for the preceding time step, calculated for each time step.

$\sum\Delta\varepsilon$ = the sum of the strain amplitude (%) contributions for each time step.

The level of dissolved oxygen in the environment was assumed to be less than 0.05 ppm, which corresponds to a low oxygen environment with an O^* equal to 0.260. As described previously, this is the conservative choice; as shown in the equation for the F_{en} in Section 3.2 of this analysis, the value for $\dot{\varepsilon}^*$ will always be negative or zero, which means that a larger value for O^* will result in a larger F_{en} .

The effects of K_e are conservatively not considered in the calculation of the F_{en} . The inclusion of K_e in the F_{en} calculation would increase the strain rates for the transients for



which K_e is greater than 1.0. However, since the environmental effects are more severe for slow transients than for fast transients, the exclusion of K_e in the F_{en} calculation is conservative. The effects of K_e are incorporated into the analysis as part of the cumulative fatigue calculation.

Using the results for the load sets for the load pairs in the fatigue table shown in Table 5-18, the F_{en} for each transient was calculated. F_{en} values were only calculated for the load pairs with a reasonably significant normal fatigue contribution (i.e. fatigue usage values ≥ 0.001). These load pairs account for roughly 97% of the cumulative fatigue usage for this location. For all other load pairs, the F_{en} was taken to be 15.35, which is the maximum value for a stainless steel material. The calculated F_{en} values for each of these load pairs are shown in Table 5-19.

Table 5-19. EAF Factors (F_{en}) for RCS Hot Leg Surge Nozzle PATH6

Load Set #	ANSYS Transient	Start (sec)	Finish (sec)	Tensile Strain ($\Delta\Sigma\epsilon$)	$F_{en} \times \Delta\epsilon$	$(F_{en} \times \Delta\epsilon)/\Sigma\epsilon$	F_{en}
25	7	0.001	752.5	0.049	0.726	14.67	7.57
26	7	842.5	3254.6	0.141	0.716	5.08	
29	7	0.001	752.5	0.049	0.726	14.67	7.69
30	7	842.5	3254.6	0.136	0.701	5.15	
33	7	0.001	752.5	0.049	0.726	14.67	7.76
34	7	842.5	3254.6	0.133	0.693	5.20	
41	7	0.001	752.5	0.049	0.726	14.67	8.34
42	7	842.5	3254.6	0.114	0.635	5.58	
45	7	0.001	752.5	0.049	0.726	14.67	8.56
46	7	842.5	3254.6	0.107	0.616	5.75	
49	7	0.001	752.5	0.049	0.726	14.67	8.80
50	7	842.5	3254.6	0.101	0.597	5.92	
57	9	0.001	1330.8	0.055	0.813	14.86	9.67
58	9	1346.5	3597.9	0.108	0.756	7.03	
37	7	0.001	752.5	0.049	0.726	14.67	7.94
38	7	842.5	3254.6	0.127	0.674	5.31	
61	10	0.001	725.5	0.034	0.497	14.76	9.57
62	10	815.5	3488.7	0.096	0.747	7.76	
8	5	1	1042.4	0.040	0.508	12.65	12.07
9	5	1044.8	1665.1	0.082	0.971	11.80	

The fatigue table from the fatigue calculation was appended to include the F_{en} results to determine the EAF results for each load pair. The summation of the EAF results for the individual load pairs represents the cumulative EAF for the RCS hot leg surge nozzle for plant operation. The total EAF was divided by the total CUF (cumulative fatigue usage without



environmental effects), resulting in the overall effective F_{en} for the hot leg surge nozzle. This calculation is shown in Table 5-20.

The CUF for the KPS hot leg surge nozzle, without environmental effects, as calculated in the fatigue analysis is 0.085. When the fatigue usage for each row in the fatigue table was multiplied by individually-calculated F_{en} values and summed, the resulting EAF is 0.7467, which is below the allowable limit of 1.0. The KPS hot leg surge nozzle EAF is therefore acceptable for the period of extended operation if plant cycle counts remain within the limits presented in Table 5-7.



Table 5-20. RCS Hot Leg Surge Nozzle EAF Results for Bounding PATH6

I	Load Set A	Load Set B	Sn, psi	Ke	Salt, ksi	n	N	Usage	F _{en}	EAF
1	13 PIO334OUT	14 PIO334OUT	65236	1.56	100410	1	1779	0.000562	15.35	0.0086
2	17 PIO331OUT	18 PIO331OUT	63946	1.4	85.709	1	3183	0.000314	15.35	0.0048
3	21 PIO321OUT	22 PIO321OUT	63601	1.3	83.993	2	3434	0.000582	15.35	0.0089
4	25 PIO304OUT	26 PIO304OUT	63021	1.3	81.134	18	3911	0.004602	7.57	0.0348
5	29 PIO285OUT	30 PIO285OUT	62382	1.3	78.032	31	4528	0.006846	7.69	0.0527
6	33 PIO275OUT	34 PIO275OUT	62050	1.2	76.436	32	4894	0.006539	7.76	0.0507
7	37 PIO250OUT	38 PIO250OUT	61233	1.2	72.565	8	6025	0.001328	7.94	0.0105
8	41 PIO200OUT	42 PIO200OUT	59667	1.1	65.353	66	9191	0.007181	8.34	0.0599
9	45 PIO175OUT	46 PIO175OUT	58922	1.1	62.024	80	11648	0.006868	8.56	0.0588
10	49 PIO150OUT	50 PIO150OUT	58210	1	58.897	639	14981	0.042653	8.80	0.3755
11	57 PIO210OUT	58 PIO210OUT	49075	1	48.984	107	37604	0.002845	9.67	0.0275
12	61 PIO177OUT	62 PIO177OUT	44013	1	44.194	102	64538	0.001581	9.57	0.0151
13	8 RCSGRP	9 RCSGRP	35727	1	38095	244	145017	0.001683	12.07	0.0203
14	3 PlntLoad	12 InadvRCSDep	31510	1	33369	1	315711	0.000003	15.35	0.0000
15	3 PlntLoad	54 PIO150HOUT	30395	1	32665	213	360657	0.000591	15.35	0.0091
16	53 PIO150HOUT	54 PIO150HOUT	30227	1	32461	135	375044	0.00036	15.35	0.0055
17	15 PIO334OUT	53 PIO150HOUT	29497	1	30817	1	522115	0.000002	15.35	0.0000
18	19 PIO331OUT	53 PIO150HOUT	29372	1	30691	1	538118	0.000002	15.35	0.0000
19	23 PIO321OUT	53 PIO150HOUT	28959	1	30269	2	595403	0.000003	15.35	0.0000
20	27 PIO304OUT	53 PIO150HOUT	28258	1	29555	18	709225	0.000025	15.35	0.0004
21	31 PIO285OUT	53 PIO150HOUT	27477	1	28758	31	866326	0.000036	15.35	0.0006
22	35 PIO275OUT	53 PIO150HOUT	27067	1	28340	32	964513	0.000033	15.35	0.0005
23	39 PIO250OUT	53 PIO150HOUT	26043	1	27295	8	1112200	0.000007	15.35	0.0001
24	43 PIO200OUT	53 PIO150HOUT	24010	1	25219	66	1439600	0.000046	15.35	0.0007
25	7 PlntUnload	53 PIO150HOUT	23554	1	25012	54	1478800	0.000037	15.35	0.0006
26	7 PlntUnload	65 Refueling	22054	1	17865	87	5973400	0.000015	15.35	0.0002
27	1 Heatup	7 PlntUnload	20540	1	17131	9	7690100	0.000001	15.35	0.0000
28	1 Heatup	4 PlntLoad	19731	1	16663	101	9086800	0.000011	15.35	0.0002
29	6 PlntUnload	59 PIO210OUT	15721	1	16421	107	9923600	0.000011	15.35	0.0002
30	6 PlntUnload	47 PIO175OUT	15206	1	16085	43	11937000	0.000004	15.35	0.0001
31	2 Cooldown	4 PlntLoad	18571	1	15442	110	17314000	0.000006	15.35	0.0001
32	4 PlntLoad	47 PIO175OUT	14820	1	14834	3	28845000	0	15.35	0.0000
33	68 OBE	68 OBE	15939	1	14345	1	47691000	0	15.35	0.0000
34	11 InadvRCSDep	47 PIO175OUT	14193	1	14054	1	169530000	0	15.35	0.0000
35	5 PlntLoad	47 PIO175OUT	13693	1	13759	33	5052300000	0	15.35	0.0000

Total = 0.084777

Total EAF= 0.7467

Total Fen = 8.807



6.0 CONCLUSIONS

ASME Code fatigue calculations for the KPS charging and RCS hot leg surge nozzles (two of the NUREG/CR-6260 sample locations) were performed, using the results of detailed, 3-D FEA. The fatigue calculations for these analyses used the methodology of Subarticle NB-3200 of Section III of the ASME Code. In evaluating primary plus secondary and peak stresses for use in the fatigue calculations, no single stress term simplifications were made. All six, unique components of the stress tensor were used throughout the evaluation to determine alternating stress intensities per the general procedure of ASME NB-3216.2 that considers varying principal stress directions.

The bounding 60-year CUF for the charging nozzle was 0.0302 using design numbers of design-severity cycles and for the RCS hot leg surge nozzle was 0.085 using 60-year projected design-severity cycles. All values are less than the ASME Code allowable value of 1.0, and are therefore acceptable for the current licensing basis if plant cycle counts are maintained within the limits analyzed herein.

60-year EAF analyses were also performed for the two nozzles per the rules of NUREG/CR-5704 [6] for austenitic stainless steels. The bounding EAF for the charging nozzle is 0.4636 using design numbers of design-severity cycles and for the RCS hot leg surge nozzle is 0.7467 using 60-year projected numbers of design-severity cycles. All EAF values are less than the allowable value of 1.0, and are therefore acceptable for the period of extended operation if plant cycle counts are maintained within the limits analyzed herein.

Considering the results of this detailed analysis using NRC approved methodology, the concerns expressed by the NRC staff in RIS-2008-30 are addressed and eliminated for the KPS charging and RCS hot leg surge nozzles.

7.0 REFERENCES

1. ASME Boiler and Pressure Vessel Code, 2001 Edition with Addenda through 2003.
2. NUREG/CR-6260 (INEL-95/0045), *Application of NUREG/CR-5999 Interim Fatigue Curves to Selected Nuclear Power Plant Components*, March 1995.
3. NRC Regulatory Issue Summary 2008-30, *Fatigue Analysis of Nuclear Power Plant Components*, December 16, 2008. United States Nuclear Regulatory Commission, Office of Nuclear Reactor Regulation.
4. NUREG-1801, *Generic Aging Lessons Learned (GALL) Report*, Revision 1.
5. VESLFAT, Version 1.42, 02/06/07, Structural Integrity Associates.
6. NUREG/CR-5704 (ANL-98/31), *Effects of LWR Coolant Environments on Fatigue Design Curves of Austenitic Stainless Steels*, 1999.
7. EPRI Technical Report TR-1012017, *Guidelines for Addressing Fatigue Environmental Effects in a License Renewal Application (MRP-47 Revision 1)*.
8. ANSYS Mechanical, Release 8.1 (w/Service Pack 1), ANSYS, Inc., June 2004 and ANSYS/Mechanical, Release 11.0 (w/Service Pack 1), ANSYS Inc., Aug 2007.
9. SI Calculation Package, *Charging Nozzle Finite Element Model*, Revision 0, October 2009, SI File No. 0900090.301.
10. SI Calculation Package, *Loads for Charging Nozzle*, Revision 0, October 2009, SI File No. 0900090.302.
11. Kewaunee Document CN-SMT-02-29, Revision 1, *Kewaunee RTSR / 7.4% Up-rating – Reactor Coolant Loop (RCL) and Pressurizer Surge Line Evaluation*, November 2003, SI File No. 0900090.201.
12. Westinghouse Document No. WCAP-16040-NP, *NSSS and BOP Licensing Report*, February 2003, SI File No. 0900090.201.



13. *Materials Reliability Program: Thermal Cycling Screening and Evaluation Model for Normally Stagnant Non-Isolable Reactor Coolant Branch Line Piping with a Generic Application Assessment (MRP-132)*, EPRI, Palo Alto, CA, 2004. 1009552. EPRI licensed material (PROPRIETARY).
14. *Materials Reliability Program: Management of Thermal Fatigue in Normally Stagnant Non-Isolable Reactor Coolant System Branch Lines – Supplemental Guidance (MRP-146S)*, EPRI, Palo Alto, CA, 2008. 1018330. EPRI licensed material (PROPRIETARY).
15. SI Calculation Package, *Stress Analysis of Charging Nozzle*, Rev. 0, October 2009, SI File No. 0900090.303.
16. SI Calculation Package, *Charging Nozzle Fatigue Analysis*, Rev. 0, November 2009, SI File No. 0900090.304.
17. SI Calculation Package, *Hot Leg Surge Nozzle Finite Element Model*, Rev. 0, October 2009, SI File No. 0900090.306.
18. Westinghouse Document No. WCAP-12841, *Structural Evaluation of the Kewaunee Pressurizer Surge Line, Considering the Effects of Thermal Stratification*, March 1991, PROPRIETARY, SI File No. KPS-06Q-201.
19. Westinghouse Document No. WCAP-14950, *Mitigation and Evaluation of Pressurizer Insurge/Outsurge Transients*, February 1998, PROPRIETARY, SI File No. 0801125.206P.
20. SI Calculation Package, *FatiguePro Analysis of Plant Data for Kewaunee Power Station – through July 2006*, Revision 0, SI File No. FP-KNPP-301.
21. Westinghouse Calculation Note No. WPS-07-32, *NSP/WPS Surge Stratification Fatigue*, SI File No. 0900090.201.
22. SI Calculation Package, *Hot Leg Surge Nozzle Loads, Reanalysis*, Revision 0, April 2010, SI File No. 0900090.321.

23. SI Calculation Package, *Hot Leg Surge Nozzle Fatigue Analysis*, Revision 0, December 2009, SI File No. 0900090.309.
24. SI Calculation Package, *Hot Leg Surge Nozzle Fatigue Analysis, Reanalysis*, Revision 0, April 2010, SI File No. 0900090.323.
25. SI Calculation Package, *Hot Leg Surge Nozzle Stress Analysis, Reanalysis*, Revision 0, April 2010, SI File No. 0900090.322.
26. SI Calculation Package, *Reactor Coolant System Run Piping Interface Loads for Charging and Hot Leg Surge Nozzles*, Revision 0, November 2009, SI File No. 0900090.311.
27. Westinghouse Systems Standard 1.3.F, *Nuclear Steam Supply System, Reactor Coolant System Design Transients for Standard Plants with Model F Steam Generators*, July 1978, PROPRIETARY, SI File No. PI-05Q-229P.
28. Westinghouse Systems Standard 1.3.X, *Nuclear Steam Supply System, Auxiliary Equipment Design Transients for All Standard Plants*, September 1978, PROPRIETARY, SI File No. PI-05Q-229P.
29. Kewaunee License Renewal Project Technical Report KLR-1302, *Metal Fatigue of the Reactor Coolant Pressure Boundary Aging Management Program*, Revision 2, July 3, 2009.

